Monetary Policy and the Term Structure of Credit Spreads

JUSTIN C. CHAN* AND MARTI G. SUBRAHMANYAM†

March 2026

Abstract

How does monetary policy affect the cost of private borrowing, as reflected in corporate credit spreads across credit ratings and maturities? We answer this question by documenting three key stylized facts for investment-grade corporate bonds. First, tighter monetary policy rates cause average credit spreads to widen significantly more than the change in average Treasury yields, thus accentuating the effects on the cost of capital. Second, the sensitivity of credit spreads to monetary policy shocks increases with the issuer's credit risk. Third, this sensitivity declines with bond maturity. To rationalize these patterns, we develop a Merton-style structural model of debt with a stochastic short rate. Interpreting innovations in the short rate as monetary policy shocks, we show that these shocks must be sufficiently negatively correlated with innovations to the firm's value process to generate the observed effects. Finally, we identify a three-factor structure of credit spreads, which we employ in a novel *Latent SVAR* framework to improve the efficiency of estimating the dynamic causal effects of monetary policy shocks on credit spreads.

JEL Codes: C58, E43, E44, E52, G12, G17.

Keywords: Credit spreads, impulse response functions, Latent SVAR, Merton model of debt, monetary policy shock, term-structure models.

*New York University, Department of Economics, 19 West Fourth Street, 10012, New York, j.chan@nyu.edu.

†New York University, Leonard N. Stern School of Business and NYU Shanghai, Kaufman Management Center, 44 West Fourth Street, 9-68, 10012, New York, msubrahm@stern.nyu.edu.

1 Introduction

A key insight in monetary economics is that monetary policy influences not only the cost of public borrowing but also that of private borrowing. While private borrowing matters for both households and firms, it is the latter that drives economic growth through aggregate investment. For many large firms, variations in borrowing costs can be observed through changes in riskless yields and in their credit spreads. The credit spread is the difference between the yield on their debt issuance and that of an equivalent-maturity safe security, typically a Treasury bond. Hence, the sum of the safe yield and the credit spread approximates the total cost of debt capital for the firm. These credit spreads reflect both the borrower's ability to repay and investors' willingness to lend given the risk of default and recovery, both of which can be affected by monetary policy. Monetary policy can influence credit spreads through multiple channels. Changes in policy rates directly affect discount rates, thereby altering the present value of existing debt and the value of collateral available for future borrowing. Policy-induced changes can also affect the projected real cash flows of the firm, influencing its capacity to service debt. Beyond these direct effects, different macroeconomic environments may shift investor risk preferences, inducing either a "reaching-for-yield" effect or a "flight-to-safety" effect, reflecting changes in perceived risk (Becker and Ivashina, 2015; Adrian et al., 2019). Thus, collectively, these channels can modify a firm's borrowing costs relative to the underlying safe rate—that is, its credit spread.

A complementary perspective of how interest rates affect credit spreads comes from structural models of corporate debt, which frame debt pricing in terms of the underlying value of the firm. In the canonical Merton model (1974), a firm's debt is represented as a portfolio consisting of a risk-free bond and a short put option on the firm's asset value. Typically, the basic model assumes zero-coupon debt that can default only at maturity if the firm's asset value falls below its obligations. This non-linear payoff structure requires inputs analogous to those in the Black-Scholes-Merton options framework: the initial value of the firm, the short-term interest rate, the volatility of the firm's asset value, the debt's maturity, and its principal.[1] The firm's value is often

[1]Equity can also be interpreted as a call option on the firm's assets, with the strike price equal to the promised

modeled as a geometric Brownian motion, while the short rate is typically assumed constant. Under this framework, a higher short rate increases the risk-neutral drift of the firm's value and reduces the present value of debt obligations. Consequently, the probability of default decreases under high interest rate regimes, resulting in lower credit spreads.

However, treating the short rate as exogenous limits the model's ability to capture dynamic responses to transitions from low to high interest rate environments. To analyze the effects of monetary policy shocks on corporate debt pricing, it is, hence, necessary to model the short rate endogenously as a stochastic process. In this paper, we extend the Merton framework by allowing innovations in the short-term interest rate to be correlated with innovations in the firm's asset value. We interpret these innovations as unanticipated shocks arising from monetary policy surprises. We further introduce the Malliavin derivative of credit spreads with respect to these shocks as a key mathematical quantity, showing that this captures the impact of monetary policy on firm value beyond the standard discounting channel. This approach also allows us to integrate insights from the literature on monetary policy and asset pricing. For instance, Bernanke et al. (1999) show that contractionary policy can increase financial frictions, reducing the value of collateral and raising monitoring costs which, in turn, increases firms' borrowing costs. In our model, this effect can be represented by a sufficiently negative correlation between monetary policy shocks and shocks to firm value.

Meanwhile, one severe limitation to the identification of the causal effects of monetary policy for the cost of private borrowing is that monetary policy is, for the most part, endogenous. In the U.S., changes in the Federal Funds rate target, the intervention rate, are motivated by the Federal Reserve's dual mandate of low unemployment and stable inflation, macroeconomic conditions that also affect the ability of firms to repay and the willingness of investors to lend. For example, economic recessions typically induce an expansionary monetary policy response by the Federal Reserve in order to reduce unemployment, while at the same time may lead to higher credit spreads due to higher default probabilities. This negative correlation between the central bank's policy rate and credit spreads may prevail in the data despite the fact that a policy tightening may

payment to bondholders.

actually cause higher credit spreads overall by making the availability of loanable funds scarcer.

To address this endogeneity, we test the predictions of our model with monetary policy surprises—the *unanticipated* component of policy that is orthogonal to information available to investors at the time of the announcement. Using a range of existing time series of such surprises, we reconstruct the dynamic causal impact of monetary policy on the term structure of Treasury yields and, by extension, on the term structure of corporate credit spreads. While Treasury yields are directly observable, credit spreads must be inferred from corporate bonds with comparable credit characteristics. To this end, we carefully clean and process all corporate bond transactions available in TRACE (Trade Reporting and Compliance Engine) from FINRA (Financial Industry Regulatory Authority) from 2002 onward, resulting in a sample of over 60,000 unique issuances. This makes our study one of the largest to date in terms of corporate bond coverage and provides a comprehensive basis for analyzing the response of credit spreads to unanticipated monetary policy shocks.

From this dataset, we estimate impulse response functions (IRFs) of credit spreads to a monetary policy shock using two methods. Our first relies on local projections (LPs) —regressions of credit spreads of a particular credit rating and maturity at some future time horizon on the current period monetary shock, controlling for prior realizations of Treasury yields and credit spreads. These projections show that for all combinations of credit ratings and maturities in our sample, the contemporaneous effect of a positive monetary policy shock is that the credit spread increases. To test whether the magnitude of this response additionally depends on the credit rating or the maturity of the credit spread, we furthermore run a pooled regression with the appropriate set of dummy variables. In general, one should expect that the responsiveness of credit spreads to monetary policy depends on both the nature of the borrower and the terms of borrowing. In our study, we find that credit spreads widen on average by approximately 10 basis points in response to a standard-deviation contractionary monetary policy shock and that this widening is more pronounced for issuances of shorter maturity and for those with a lower credit rating. For example, this same one-standard-deviation shock causes an increase in the ballpark of 20 basis points for triple-B-rated, short-maturity credit spreads, but less than 5 basis points for triple-A and double-A, long-maturity credit spreads.

We demonstrate that these stylized facts accord with the predictions of our model precisely when the correlation between monetary policy shocks and firm value shocks is sufficiently negative.

Since the credit spreads representative of a particular credit rating and maturity are measured with substantial noise, we then attempt, in our second method, to improve the efficiency of our time series estimation by leveraging information found in the cross-section of credit spreads. In a canonical paper, Nelson and Siegel (1987) show that a three-factor model in which the factor loadings are functions of the maturity of the Treasury yield and a decay parameter leads to a remarkably good fit of Treasury yield data. These factors have the interpretation of a level, slope, and curvature based on how the factor loadings vary across maturities. Analogously, we demonstrate here that three factors also capture a substantial proportion of the variation in the term structure of credit spreads for various credit ratings across investment-grade bonds. We additionally show that these factors can similarly be viewed as a level, slope, and curvature.

Inclusion of these factors in a local projection should improve the efficiency of estimation of the IRFs, as it can control for persistence in the cross-sectional variation in yields and credit spreads. The issue, however, is that these factors are unobserved, and estimating them separately from the data leads to the problem of generated regressors. To address this concern, we identify conditions under which the impulse response functions constructed from regression coefficients in this infeasible LP coincide with those implied by a state-space model. Here, the monetary policy surprise and the latent factors jointly form a state transition equation that is identified through the measurement equation, which ties the latent factors to observed yields and spreads. This finding is similar to the equivalence result between local projections and structural vector autoregressions (SVARs) presented in Plagborg-Møller and Wolf (2021). Consequently, we describe this procedure as a Latent SVAR identification strategy, in acknowledgment of the fact that the SVAR of interest in our model, which determines how the monetary policy shocks and the latent factors co-vary over time, is unobserved. We demonstrate that this second approach of estimating the IRFs from a Latent SVAR leads a marked reduction in the standard errors of our IRF estimates and imply more persistent effects from monetary shocks, a finding that is otherwise obfuscated in the LP setting.

1.1 Related Literature

This paper relates to a large literature examining the effects of monetary policy on asset prices and risk premia. Early contributions such as Cook and Hahn (1989) document the response of nominal interest rates to monetary policy announcements, while Bernanke and Kuttner (2005) study the transmission of monetary policy to equity prices. Later, Hanson and Stein (2015) analyze the response of real interest rates and term premia to policy interventions. Collectively, these studies establish that monetary policy affects not only expected short rates but also risk premia embedded in asset prices. Our paper contributes to this literature by focusing specifically on corporate credit spreads and by studying their response across both the maturity and credit-rating dimensions.

A closely related strand emphasizes how monetary policy shapes the price of risk and risk-taking behavior through financial frictions. Drechsler et al. (2018), for example, argue that higher policy rates tighten intermediary balance-sheet constraints, forcing intermediaries to reduce holdings of risky assets and thereby increasing risky yields. In their framework, contractionary monetary policy raises the price of risk via intermediary net worth. Earlier work by Gilchrist and Zakrajšek (2012) decompose corporate bond spreads into expected default components and an excess bond premium, showing that the latter captures time-varying risk compensation and predicts macroeconomic activity. Gertler and Karadi (2015) embed such credit spread measures into an SVAR framework and document that monetary policy shocks significantly affect credit spreads and real activity. The macroeconomic relevance of credit spread heterogeneity is further underscored by Ottonello and Winberry (2020), who show that highly rated firms—whose credit spreads respond least to monetary policy shocks—exhibit the strongest investment responses. Together, these contributions highlight that monetary policy influences borrowing costs through credit market frictions and risk premia. Although we do not directly examine real outcomes, our results provide a structural interpretation of how monetary policy shocks reshape the cross-section and the term structure of the cost of credit of firms, thereby complementing this literature on monetary transmission and cross-sectional heterogeneity in corporate bond markets.

On the theoretical side, our structural framework draws inspiration from the seminal model of

corporate debt by Merton (1974), which views risky debt as a contingent claim on firm value. This Merton framework has been extended in numerous directions, including the modeling of fixed and floating-coupon debt (Longstaff and Schwartz, 1995), optimal default (Leland and Toft, 1996), and multi-factor hazard rates (Jarrow et al., 1997).[2] We present a credit-pricing model with stochastic interest rates that is closest in spirit to Shimko et al. (1993), which combines the Merton model with the simple Vasicek interest rate process. Our focus differs, however, in that we interpret innovations in the short rate process as unanticipated monetary policy shocks and evaluate the Malliavin derivative of credit spreads with respect to these innovations. This allows us to quantify how monetary policy shocks propagate to firm value and corporate bond yields beyond the standard discounting effects, thereby linking structural credit risk modeling directly to monetary policy identification.

Our paper also relates to the empirical literature on the joint behavior of Treasury yields and corporate bond spreads. Duffee (1998) documents a negative correlation between changes in Treasury yields and changes in credit spreads, a result echoed by Collin-Dufresne et al. (2001). These patterns are frequently interpreted through portfolio reallocation mechanisms: during "flight-to-safety" episodes, Treasury yields decline while credit spreads widen as investors substitute away from risky credit to safe debt, whereas "reaching-for-yield" episodes generate the opposite co-movement. However, these studies are largely reduced-form and do not establish a causal link between monetary policy shocks and credit spreads. By using monetary policy surprises as our regressor of interest, we provide causal evidence that an unanticipated tightening raises credit spreads even as Treasury yields increase, consistent with a contraction in firm value and tighter lending conditions.

More generally, our identification strategy builds on the high-frequency monetary policy literature starting with Kuttner (2001) and Gürkaynak et al. (2005), which exploit changes in short-rate futures within narrow windows around Federal Open Market Committee (FOMC) announcements to isolate unanticipated policy components. It is believed that within this window, no other shock is likely to affect these rate movements and, thus, they reflect solely the changes due to monetary policy. This distinction between unanticipated and systematic components is central for causal

[2]For a more comprehensive review of the developments in credit pricing as it pertains to optimal liability and capital structure, see Sundaresan (2013).

inference. The predictable component of the policy rate is endogenous to economic conditions and reflects the central bank's reaction function. In contrast, the unanticipated component can be viewed as plausibly exogenous variation in monetary policy.

However, a key development in this literature is the recognition that announcement-window surprises may reflect both a pure monetary policy component and a central bank information component. To address this, Jarociński and Karadi (2020) use sign restrictions to decompose high-frequency surprises into a pure monetary policy shock — the exogenous shift in policy stance — and a central bank information shock, which captures information revealed by the central bank about its assessment of economic fundamentals. This distinction is important because the information component can generate asset price movements that are positively correlated with macroeconomic news, potentially confounding causal inference if not separated from the true policy shock and its effects. Meanwhile, Miranda-Agrippino and Ricco (2021) offer an alternative approach by projecting high-frequency surprises onto revisions in internal Federal Reserve Greenbook forecasts of output and inflation and using the residual component as the shock measure. Similarly, Bauer and Swanson (2023b) orthogonalize high-frequency surprises with respect to publicly available macroeconomic expectations contained in the Blue Chip Economic Indicators, thereby removing predictable components embedded in the announcement response. More recently, Acosta et al. (2025) refine the identification further by distinguishing between surprises measured around the FOMC statement release and those measured during the subsequent press conference. This decomposition recognizes that markets may update differently in response to the formal policy decision and to forward-looking communication by the Chair. We consider a variety of these measures to ensure that our results are robust to different specifications of monetary policy shock.

Methodologically, our empirical specification builds on the extensive literature modeling the term structure of interest rates using low-dimensional factor representations. Nelson and Siegel (1987) introduce a three-factor representation—level, slope, and curvature—that provides a parsimonious and accurate fit of Treasury yield data. The ability of three factors to capture most of the yield variation is documented by Litterman (1991), who shows that the first three principal

components explain a large fraction of Treasury yield movements. Later, Diebold and Li (2006) demonstrate that modeling the dynamics of the Nelson-Siegel factors substantially improves yield curve forecasts, while Diebold et al. (2006) show how the framework can be embedded in a state-space system and estimated via the Kalman filter. More generally, affine term-structure models are analyzed in detail by Duffie and Kan (1996), and Joslin et al. (2011) study inference under no-arbitrage restrictions. Importantly, Ang and Piazzesi (2003) integrate macroeconomic variables directly into an affine term-structure model, demonstrating that macroeconomic shocks play a central role in driving the Treasury yield curve. More recently, alternative approaches to term-structure modeling emphasize market segmentation and preferred habitat effects. Vayanos and Vila (2021) develop a model in which arbitrageurs with limited risk-bearing capacity intermediate supply and demand imbalances across maturities, generating time-varying term premia. While our approach does not model market segmentation explicitly, our findings that monetary policy shocks affect the term structure of credit spreads are consistent with mechanisms in which financial frictions and intermediary constraints shape risk premia across maturities.

Our approach instead extends the Nelson–Siegel tradition in two directions. First, we jointly model the latent factors for Treasury yields and credit spreads, imposing a Nelson–Siegel structure to capture economically motivated smoothness across maturities and rating categories. Second, rather than focusing on forecasting performance, we use the factor structure for structural identification and causal inference. In this sense, our framework can be viewed as a restricted state-space model or dynamic factor model in the spirit of Stock and Watson (2016), where the latent factors are the states which follow autoregressive processes and the yields and spreads are the observations that load linearly on those factors. We show that Nelson–Siegel restrictions suffice to identify the system matrices of this model, while the identification of impulse responses can be achieved by ordering the monetary policy shock first as a factor and applying a Cholesky decomposition of the state covariance matrix.

Our empirical strategy also draws on the local projection methodology of Jordà (2005), which provides a flexible approach to estimating IRFs without imposing the full dynamic structure of a

VAR. Local projections estimate horizon-specific regressions directly, thereby avoiding potential misspecification of the underlying state dynamics. However, obtaining efficient causal estimates necessitates a robust set of controls. Given the high degree of multicollinearity among yields and spreads, these controls should take the form of a parsimonious, low-dimensional representation such as lags of the underlying term-structure factors. These, however, are not directly observed, and so we can only construct an approximate set of controls to run our local projections. Alternatively, an equivalent approach would be to identify the IRFs using the state-space model described previously. Recent work by Plagborg-Møller and Wolf (2021) detail the general conditions under which LPs and SVARs identify the same IRFs. We builds on these insights and provide conditions under which equivalence holds when the SVAR is latent. In this sense, our approach unifies LPs, SVARs, and state-space models within a single coherent framework motivated by traditional affine term-structure models.

1.2 Roadmap

The remainder of the paper is organized as follows. Section 2 develops an arbitrage-free model of credit spreads and interest rates under the risk-neutral measure and identifies the determinants of the response of credit spreads to monetary policy shocks. Section 3 describes the calculation of aggregate credit spreads across credit ratings and maturities and provides initial evidence using LPs that they widen following a contractionary monetary policy shock and that this widening further depends on the credit quality and maturity of the issuance. Finally, Section 4 describes the factor structure of credit spreads to motivate the introduction of a Latent SVAR to improve the efficiency of estimating the dynamic effects of monetary policy shocks.

2 Monetary Policy Shocks in a Merton-Style Model of Credit Spreads

This section extends the classic Merton (1974) model of corporate debt by allowing the short rate process to be stochastic and by permitting correlation between innovations in interest rates

and firm value. As is similarly analyzed in Shimko et al. (1993), the short rate here is given by a simple one-factor model, namely the Vasicek model in which the stochastic differential equation for the short rate is a Ornstein-Uhlenbeck process (Vasicek, 1977).[3] However, in a significant departure from previous models presented in both the term structure literature and the derivatives pricing literature, including the ones cited above, we additionally ascribe economic meaning to the sources of stochasticity. More specifically, in our model, the outcome of the Brownian motion in the interest rate process has the structural interpretation of a monetary policy shock. This allows us to comment on how an unexpected monetary policy tightening can affect credit spreads and provides us with intuition as to how and why the magnitude of this response in corporate credit markets can vary by the volatility of the firm's assets and by the maturity of the debt issuance.

In what follows, we work directly with the evolutions of both the value of the firm and the short rate under the risk-neutral measure $\mathbb{Q}$. Let $(\Omega,\mathcal{F},\mathbb{Q})$ be the associated probability space endowed with the filtration $\{\mathcal{F}_t\}_t$. The value of the firm V_t, which can be thought of as the market value of its assets, is defined on this space by the geometric Brownian process:

$$dV_t = r_t V_t dt + \sigma_V V_t dW_t^V, \tag{1}$$

where r_t is the instantaneous short rate at time t, and $\sigma_V > 0$ is the asset volatility, which is taken as exogenous. Observe that in the absence of arbitrage, the drift of this process must be pinned down by the short rate. This short rate meanwhile follows a Vasicek process,

$$dr_t = \kappa(\theta - r_t)dt + \sigma_r dW_t^r, \tag{2}$$

with $\kappa > 0$ being the rate at which this process reverts to the long-run mean θ, and $\sigma_r > 0$, being the

[3]We choose to model the (single-factor) short rate process rather than a more complex formulation of the whole term structure of interest rates (such as all forward rates in the Heath-Jarrow-Morton framework (1992)) for several reasons. First, the main instrument of monetary policy interventions is the short rate, other than in special cases such as quantitative easing and yield curve control. Second, this choice makes the model more tractable in deriving a closed-form solution for credit bond prices and the credit spread. Third, the empirical implications of the model are made clearer with fewer parametric assumptions.

volatility of the short rate process. Through endogenizing the interest rate, we can interpret these parameters as potentially being set by a combination of market forces and the central bank. For example, one may view κ and σ_r as being fundamentally determined by market characteristics such as liquidity, as well as the risk aversion and investment horizon of market participants. Meanwhile, θ is a systematic target rate set by the monetary authorities.[4] Our main focus, however, is on the Brownian motion term dW_t^r, which we view as conceptualizing monetary policy shocks, the unanticipated component of monetary policy that drives interest rates. That said, clearly, there are other possible sources of stochasticity in the interest process such as market microstructure noise. For our purposes, we do not model them here. Instead, it suffices to think about this process as only being driven by surprises in monetary policy at least in a small time-window around the monetary policy announceent. These surprises may plausibly be correlated with the Brownian motion on the value process insofar as they induce a contemporaneous shock to the value of the firm's assets. We correspondingly denote this correlation as:

$$dW_t^V dW_t^r = \rho dt, \qquad \rho \in [-1,1]. \tag{3}$$

Following Merton (1974), let us assume that the firm issues zero-coupon debt with face value K at time t that matures at time T. We denote the value of this risky corporate debt at time t by $D_K(t,T)$, and the time until maturity as $\tau = T-t$. At maturity, the firm pays the face value in full as long as it has sufficient assets to do so; otherwise, the firm defaults on its debt and recovery is limited by the assets on hand. That is, the payoff of the debt at time T is given by $D_K(T,T) = \min(V_T,K)$. In this basic Merton framework, default is only possible at the maturity date T, as there are no intermediate payments due before maturity. Equivalently, we may rewrite this payoff as $D_K(T,T) = K - \max(K-V_T,0)$, which is also the payoff of a position in a zero-coupon bond of the same face value and maturity alongside a short put on the firm's value. Intuitively, the put is a bet on the firm's default. The more in-the-money the put is, the higher the probability of default (under the

[4]The target rate could additionally be determined by some policy rule that depended on macroeconomic factors. In this case, θ would be time-varying as is assumed in the Hull-White (1990) of the Vasicek model.

risk-neutral measure). Since default is to the detriment of the holders of the firm's debt, one can intuitively understand the debt default option as consisting of a short position on the put on firm value.

More convenient for pricing, however, is the representation of the payoff as $D_K(T,T) = V_T - \max(V_T - K, 0)$, which can be replicated by a portfolio that directly invests in the firm and a short call option of strike K on the value of the firm. By the no-arbitrage condition, the debt and the portfolio must have the same price. In other words,

$$D_K(t,T) = V_t - C_K(t,T), \tag{4}$$

where $C_K(t,T)$ is the price at time t of the call option. To calculate the credit spread on this debt, let $P(t,T)$ the price of a riskless zero-coupon bond of the same maturity, with a face value of \$1. It is well-known that affine term-structure models generate bond prices that are exponentially affine in the factors (Duffie and Kan, 1996). For the Vasicek model, this has the closed form:

$$P(t,T) = \exp\big(A(t,T) - B(t,T) r_t\big), \tag{5}$$

$$A(t,T) = \left(\theta - \frac{\sigma_r^2}{2\kappa^2}\right)\big(B(t,T) - \tau\big) - \frac{\sigma_r^2}{4\kappa} B(t,T)^2, \tag{6}$$

$$B(t,T) = \frac{1 - e^{-\kappa\tau}}{\kappa}. \tag{7}$$

The credit spread is then defined as the yield differential between the continuously compounded rates of the risky corporate bond and the riskless benchmark:

$$s(t,T) = -\frac{1}{\tau} \ln\left(\frac{D_K(t,T)}{K P(t,T)}\right). \tag{8}$$

We wish to study how this credit spread changes as a result of a one-unit surprise increase in the short rate. Under our description of the model, this can be understood as the contemporaneous effect of a monetary policy shock on the credit spread. Mathematically, this can be represented as the Malliavin derivative of the credit spread with respect to the Brownian motion on the short

rate evaluated at time t, which we denote $\mathcal{D}_t^r s(t,T)$. More formally, $\mathcal{D}_t^W$ is the differential operator defined on $(\Omega,\{\mathcal{F}_t\},\mathbb{Q})$ equipped with a Gaussian structure that, when acting on a smooth function G of random variables, measures the sensitivity of G to perturbations in the Brownian motion path W at time t. Heuristically, this can be thought of as the partial derivative of G with respect to the noise W_t at time t.[5]

For example, observe that the Malliavin derivative of the short rate r_t with respect to its Brownian motion at time t is simply given by the volatility of the process: $\mathcal{D}_t^r r_t = \sigma_r$.[6] Similarly, the Malliavin derivative of the value of the firm's assets V_t with respect to W_t^r is given by $\mathcal{D}_t^r V_t = \rho\sigma_r V_t$. Note here that the instantaneous effect of the interest rate shock on the value of the firm is through the direct correlation of the two Brownian motions. Even though the drift of the value process is determined by the short rate, this channel does not contribute to this Malliavin derivative as it is evaluated on an instantaneous change during which the realized drift is infinitesimal. The chain rule similarly applies to Malliavin calculus, and thus the Malliavin derivative of the zero coupon bond price $P(t,T)$ with respect to W_t^r is as follows:

$$\mathcal{D}_t^r P(t,T) = -B(t,T)P(t,T)\sigma^r, \tag{9}$$

where $B(t,T)$ is the Vasicek factor loading defined in Equation 7.

Finally, to combine all of this together and solve for the Malliavin derivative of the credit spread with respect to W_t^r, we must solve for the price of the corporate debt. This amounts to pricing the call option on the value of the firm with strike K, which we can do by evaluating its expected discounted payoff under the risk-neutral measure. This is directly analogous to the Black-Scholes-

[5]This is distinct from Itô calculus which formalizes the differential along the evolution of stochastic processes in time. Malliavin calculus, meanwhile, provides a mathematical representation for the differential across paths in probability space along the direction of a Gaussian perturbation. For a rigorous and thorough treatment of the topic of Malliavin calculus and its applications, particularly in mathematical finance, see Nualart (2006).

[6]To be more precise, we should in fact consider the Malliavin derivative of the short rate with respect to the Brownian motion for the rate process under the physical measure, $\mathbb{P}$, as that is the quantity that we can directly observe in the data. Nevertheless, it is a corollary of Girsanov's theorem that these two derivatives are the same provided that $\mathbb{Q}$ is an equivalent martingale measure of $\mathbb{P}$. Consequently, we do not make a distinction between the Malliavin derivative with respect to the Brownian motion under the physical measure and that with respect to the corresponding Brownian motion under the risk-neutral measure in the analysis that follows.

Merton value of a European call option on a stock given stochastic interest rates. We provide the results directly below, while a full derivation using a change of measure is given in Appendix A.1.[7]

$$D_K(t,T) = V_t\big(1-N(d_1^*)\big) + KP(t,T)N(d_2^*), \tag{10}$$

$$d_1^* = \frac{\ln\big(\frac{V_t}{KP(t,T)}\big) + \frac{1}{2}\int_t^T \sigma_*^2(s,T)ds}{\sqrt{\int_t^T \sigma_*^2(s,T)ds}}, \tag{11}$$

$$d_2^* = d_1^* - \sqrt{\int_t^T \sigma_*^2(s,T)ds}, \tag{12}$$

$$\sigma_*^2(t,T) = \sigma_V^2 + \sigma_r^2 B(t,T)^2 + 2\rho\sigma_V\sigma_r B(t,T), \tag{13}$$

where $N(.)$ is the cumulative density function of the standard normal distribution.

Observe that the term on the right hand side in Equation 10 reduces to the standard Black-Scholes-Merton formula for a put option when $\sigma_r = 0$, which corresponds to a deterministic short rate (Black and Scholes, 1973; Merton, 1973). Under stochastic interest rates, however, the effective volatility of the call option is determined by the Vasicek contribution $B(t,T)$ and the correlation, ρ, between the two processes. When the correlation is negative, the effective volatility of the option is lower since the asset value and the discount factor partially hedge each other reducing the uncertainty in the equity payoff.

As demonstrated in Appendix A.2, we can then calculate the Malliavin derivative of the credit spread with respect to the monetary policy shock. This is given by:

$$\mathcal{D}_t^r s_t(\tau) = -\frac{1}{\tau}\frac{V_t}{D_K(t,T)}\big(1-N(d_1^*)\big)\big(\rho\sigma_V + B(t,T)\sigma_r\big). \tag{14}$$

From Equation 14, we note that the responsiveness of the credit spread to a monetary policy shock depends on the following key terms: the time until maturity of the debt, τ; the leverage of the firm expressed as the assets to liabilities ratio, $\frac{V_t}{D_K(t,T)}$; the absolute value of the hedging ratio or the

[7]Shimko et al. (1993) offer an alternative derivation of the credit spread by solving the corresponding Black-Scholes-Merton partial differential equation formed from hedging the interest rate risk and credit risk associated with the corporate debt.

sensitivity of the debt price to the underlying, $1-N(d_1^*)$; and the effects of the uncertainty of the short rate on the value of the firm's assets and debt obligations, $\rho\sigma_V+B(t,T)\sigma_r$. On the one hand, a monetary policy shock impacts the firm's assets directly by inducing a contemporaneous change in the value by $\rho\sigma_V$. On the other hand, a monetary policy shock impacts the debt burden of the firm by altering the present value of the firm's future principal payment through the sensitivity of discount rates to this shock, $B(t,T)\sigma_r$. These two channels directly link to the probability that the firm can repay the principal at maturity. The higher the asset values and the lower the debt burden, the lower is the likelihood of default, while lower asset values and higher debt burden increases it. Since the time until maturity, leverage, and absolute value of the hedging ratio are all strictly non-negative, whether monetary policy shocks cause credit spreads to widen or narrow depends crucially on the sign of this net effect: $\rho\sigma_V+B(t,T)\sigma_r$. This in turn depends on the sign of the correlation ρ.

For example, if the correlation between the two Brownian motions is significantly negative, $\rho<-\frac{B\sigma_r}{\sigma_V}\leq 0$, then the Malliavin derivative is positive, and a positive monetary policy shock leads to higher interest rates and a contemporaneous widening of credit spreads. In the case where the correlation is zero, the result matches that in the traditional Merton model of debt, in which higher interest rates cause credit spreads to narrow as the monetary policy shock only affects the firm's distance to default through impacting the discount rate on the principal. Higher interest rates reduce the present value of debt, thus reducing the probability of the firm's default.

Why would monetary policy shocks and shocks to firm value be negatively correlated? Early literature has documented considerable evidence that the stock market values tend to fall when the central bank unexpectedly tightens interest rates (Rigobon and Sack, 2004; Bernanke and Kuttner, 2005). Potential explanations include a household consumption channel in which unexpected monetary tightening leads to less spending, which reduces the future cashflow of the firm. Alternatively, a negative correlation could manifest in the investment channel as higher interest rates lead to tighter lending conditions in which firms are unable to access capital (Bernanke et al., 1999). Another explanation could be that firm leverage become more costly when interest rates increase. Dealers intermediate trading activity less resulting in a fall in equity prices that

drive asset values down (Drechsler et al., 2018). We leave an exploration of the relative merits of each of these arguments to future research.

Conversely, monetary policy shocks and shocks to firm value may plausibly be positively correlated in the data due to an information effect (Nakamura and Steinsson, 2018). Here, monetary policy shocks may convey private information of the central bank regarding current and future macroeconomic conditions. Since expansionary policy is typically enacted in response to economic downturns and contractionary policy in response to economic booms, unexpected loosening or tightening of policy may imply a better or worse than expected economy, which in turn may lead to a narrowing or widening of credit spreads respectively. Alternatively, the measurement of the shock may not truly capture exogenous variation and is instead contaminated with the systematic response of the central bank to economic news (Bauer and Swanson, 2023a). Given this, it is evident that the methodology used to construct the monetary policy shock in light of the possible correlations will have a significant impact on the estimated responses of credit spreads.

Additionally, our derivation of the Malliavin derivative suggests that the sensitivity of credit spreads to monetary policy shocks is conditional on both asset volatility and debt maturity. As demonstrated by the partial derivatives in Appendix A.3, for firms with sufficiently low leverage, when ρ is such that a positive interest rate shock induces a widening of the credit spread, this response is magnified by the volatility of the underlying value process σ_V. Within the investment-grade universe, where such leverage conditions are typically satisfied, our model thus predicts that the widening of spreads following a contractionary monetary shock will be systematically more pronounced for lower-quality issuers. Meanwhile, the relationship between spread sensitivity and maturity τ is more nuanced. While the sign of the partial derivative $\partial \mathcal{D}_t^r s_t(\tau)/\partial\tau$ is generally indeterminate due to competing duration and convexity effects, the asymptotic behavior remains clear. As demonstrated in Appendix A.4, the Malliavin derivative vanishes as maturity approaches infinity, rendering the credit spread on ultra-long-dated debt virtually unresponsive to spot-rate shocks. Intuitively, even if a monetary shock reduces contemporaneous firm value, the impact on the cumulative probability of default is negligible when the time to expiry tends to infinity. Consequently, we

expect the responsiveness of corporate bond spreads to follow a "hump-shaped" or decaying term structure, where the most significant impacts are concentrated in short- and medium-dated issues.

To summarize, while our model of credit spreads is agnostic as to how the shocks to firm value are correlated with the monetary policy shocks, it allows us to generate three testable implications on the causal relationship between monetary policy and credit spreads, which we explore further in the following sections where we estimate the IRFs of various credit spreads to a monetary policy shock. These implications concern the fact that the causal effects of monetary policy on credit spreads will differ in magnitude, and potentially sign and significance, depending on the characteristics of the credit spread and how the measurements of monetary policy shocks are correlated with firms' asset values. We list these three hypotheses below:

1. A contractionary monetary policy shock that is negatively correlated with asset values may induce a positive response in credit spreads (widening) if the correlation is significantly negative, whereas it will induce a negative response (narrowing) if the correlation is positive.

2. A contractionary monetary policy shock that is negatively correlated with asset values accentuates the sensitivity of credit spreads to monetary policy shocks for weaker credit ratings.

3. A contractionary monetary policy shock that is negatively correlated with asset values may attenuate the sensitivity of credit spreads to monetary policy shocks for spreads of longer maturities.

We proceed by explaining how we compute these credit spreads from transactions data on corporate bonds before testing each of the three hypotheses above.

3 Data and Stylized Facts on Credit Spreads and Their Responsiveness to Monetary Policy Shocks

3.1 Computation of Aggregate Credit Spreads

We begin by assembling a panel of corporate bond yields in which each element in the panel is assumed to be a representative yield to maturity for a bond of a given credit rating and maturity

category, at that point in time. Using the population of bond issues in the Mergent FISD database, we selectively apply the following filters to derive our sample. First, we restrict our sample to consist of only senior unsecured debt with a fixed coupon rate. This set includes corporate debentures, corporate medium term notes, and corporate paper. Second, to avoid complications with exchange rates, we consider only issuances that are denominated in US dollars from companies domiciled in the United States. Moreover, we limit the sample to issues that are not offered globally; that is, we focus on issues that are only traded in US markets. Third, using data on bond redemptions, we can identify issuances with embedded optionality such as callable, puttable, exchangeable, convertible, and redeemable bonds. Despite these bonds making up a considerable fraction of the universe of corporates, we drop such bonds since their embedded optionality means that they will offer a higher or lower coupon yield on average (depending on the optionality) when traded at par compared to a vanilla fixed-rate corporate with the same payment dates. Moreover, the value of the optionality is time-varying, which would complicate matters further in our exercise to extract the term structure of credit spreads. While some data vendors such as Bloomberg offer data on option-adjusted credit spreads, the methodology behind the computations is proprietary and hence opaque and non-replicable to researchers. For these reasons, we remove such bonds from our sample.

Fourth, we exclude bonds that have either been issued under additional structuring or have undergone some change in their structuring during their lifetime. For example, with regard to the former, we omit secured-lease obligations, bonds that are payable-in-kind, asset-backed issuances, debt that was issued under SEC rule 144a or were privately placed, debt that was sold as part of unit deal, contracts with protective covenants such as asset sale clauses or security pledges, and preferred securities. With regard to the latter, we omit bonds that have had changes to its coupon frequency, have defeased, or have defaulted. Additionally, using bankruptcy data, we drop observations for issuers whose borrowing became restricted or who filed under Chapter 11. Finally, since our data on corporate bond transactions starts only in July 2002, we keep only the bonds that are active past this point in time. The result is a sample of 63,296 unique issuances. While this sample is much smaller than the original population size as a result of various omissions

(approximately one-tenth in size), it remains larger than most samples used in studies of corporate bonds and exhibits substantial variation in credit rating and maturity.[8]

Using this cleaned sample, we match the corporate bond identifiers (CUSIPs) with the population of executed trades data for corporate bonds in the TRACE Enhanced File, which dates from July 2002 to March 2025. We focus on transactions that take place within the secondary market as these are the trades that are most likely to contribute to price discovery. Pricing in the secondary market is competitively driven by fluctuations in demand and supply, which are, in turn, influenced by the interest rate environment, credit risk, and investor sentiment (Bessembinder and Maxwell, 2008; Friewald et al., 2012). Pricing in the primary market, meanwhile, is less transparent and is often driven by the incentives of underwriters to attract investment and ensure the deal closes. This may mean that new issues are made at a discount that would not otherwise reflect prevailing market prices.

In addition, as noted previously in the literature, transactions data from TRACE include reports of trade cancellations and corrections. In such circumstances, the original report remains available in the data even though it does not reflect the true terms of conditions under which the trade was actually executed, if executed. Following the procedure in Dick-Nielsen (2014), we match trade cancellations and trade reversals with their original reports and delete all matches from the dataset, while for matched trade corrections and original reports, we keep only the trade corrections and drop the original reports. Additional care is also taken in the case of trade correction cancellation reports existing in the dataset. Moreover, for inter-dealer trades, a report will be submitted for both the buy-side and the sell-side. We correct for duplicates and keep only one of the reports in our sample.

With this cleaned dataset of transactions, we then construct a volume-weighted average price (VWAP) for each issuance traded in the day.[9] Utilizing Mergent FISD data on issuance characteris-

[8]By comparison, one of the most comprehensive studies of corporate bond liquidity that uses TRACE transactions data has a sample size of 23,703 bonds and 3,261 firms (Friewald et al., 2012).

[9]In fact, we take additional care in defining a day not in terms of calendar date from opening bell to closing bell of the market but instead as starting and ending at the time of the scheduled FOMC announcements. This helps to ensure that on the date of the FOMC announcement, all transactions recorded for that day did indeed occur after the announcement. Since, however, we later aggregate these daily observations into periodic observations where an observation period is defined as the time between consecutive FOMC meetings, this procedure of ensuring exact alignment at the daily frequency is arguably of secondary significance. FOMC announcement dates and

tics such as coupon rate, maturity date, payment frequency, and daycount convention, we can then back out a yield-to-maturity associated with the VWAP of each transacted CUSIP per day in our sample. Using this cleaned sample, we then use historical and current ratings data to match each transacted CUSIP with their latest rating. There are three credit ratings agencies that we focus on: Fitch's, Moody's, and Standard and Poor's (S&P). While a bond remains active, it may be re-rated several times both across different agencies, and often within the same agency. Consequently, we assume that the most recent credit rating for a bond reflects the most up-to-date information regarding its credit risk.[10] The ratings may occur after the bond has matured, often for the purposes of default and recovery analysis, or to provide further details in litigations and disputes. As mentioned previously, we omit transactions of a bond that occur after that bond's maturity. By extension, we ignore ratings that occur after the bond has matured. Building on these ratings, we bucket each transaction into various ratings categories for investment-grade bonds: Prime and High Grade corporate bonds (AAA to AA-), Upper Medium (A+ to A-), and Lower Medium (BBB+ to BBB-).[11]

Given a particular credit rating category, we then bin each transaction based on a partition of the tenor space and calculate the median yield for each bin. Our partition consists of varying interval lengths given by: 0.5-1.5, 1.5-2.5, 2.5-3.5, 3.5-4.5, 4.5-5.5, 5.5-8.5, 8.5-11.5, 11.5-16.5, 16.5-23.5, 23.5+. These intervals are centered on the years: 1, 2, 3, 4, 5, 7, 10, 14, 20, 30. Note that we throw out bonds that have less than half a year before maturity since these often trade at particularly volatile prices. As is standard practice, this approach uses a finer division to capture

times are all collected from the U.S. Monetary Policy Event-Study Database as described in Acosta et al. (2025).

[10] One concern may be that the changes in a bond's credit rating over time may reflect as much the changes in appraisal standards and regulatory effects on ratings agencies as it does on the changes in the intrinsic credit-worthiness of the bond. A discussion of this topic can be found in Bolton et al. (2012). To the extent that these changes are typically both sudden and spaced apart in time, this should not heavily bias our study of the comparatively short-term effects of monetary policy on credit spreads across credit rating categories.

[11] We ignore high yield bonds - that is, bonds rated BB+ and below on the S&P grading scale or its equivalent - as there is significant heterogeneity in credit quality within this sector of the corporate bond market. Moreover, this is a highly illiquid market as many large mutual funds, pension funds, and insurance companies are prohibited from having such bonds in their holdings, and thus do not deal in this market. Consequently, it is also not possible to address this heterogeneity by subdividing the credit rating into finer categories. Doing so would create significant missing data issues in our sample, and even when data are not missing, the computed bond yields are likely to be unreliable as a representative bond yields for that credit rating class and maturity, since their computation is likely be based on very few observations for that day. A similar argument applies in the consideration of finer aggregation schemes such as categorizing at the credit rating and industry level.

variation in the short end of the corporate bond curve and then gradually adjusts the interval lengths wider as the tenor increases. The median yield is then taken to be the representative yield to maturity of a bond with maturity equal to the center of the interval. Here, we use the median yield rather than the mean since we observe that there is significant noise in the data that persists even after the cleaning procedure has been applied. For example, mistakes in reporting the price of a transaction such as the erroneous change to a particular digit will not easily be picked up by the cleaning procedure if no trade correction report was made. The median in this setting allows us to ensure greater robustness with respect to such errors provided we have a large enough subsample in each tenor interval for each credit rating.

Table 1 below presents some key summary statistics for our sample of daily aggregated corporate bonds yields during the period between June 2002 and March 2025. As is to be expected, the median yields are increasing in tenor and decreasing in creditworthiness. The opposite is true when we look at dispersion: The standard deviation in yields is decreasing in tenor and increasing in creditworthiness. These simple observations suggest that the term structure of corporate bond yields across credit ratings inherits some key features from the term structure of Treasury bond yields, namely that it is, on average, upward-sloping and the short-end is more volatile than the long-end. In the Appendix, Figure 5 also presents the number of unique corporate bonds that are transacted in our sample for each credit rating and tenor category. The counts for these are also decreasing in tenor, partly because liquidity generally declines with maturity. This is also a somewhat mechanical effect since a long-dated bond may be transacted several times during its lifetime and so will be recorded as a unique CUSIP every time its tenor crosses a threshold. This same reasoning also explains why the number of unique issuers per credit rating and tenor category is decreasing in tenor. We additionally note that a significant majority of unique CUSIPs that make up our sample are Upper Medium Grade bonds.

We then take constant-maturity yield data for U.S. Treasuries from the FRED website for the following maturities: 1M, 3M, 6M, 1Y, 2Y, 3Y, 5Y, 7Y, 10Y, 20Y, and 30Y. These yield data are constructed using market quotes collected towards the end of the trading session, when

Table 1: Summary Statistics for Daily Corporate Bond Yields

	1Y	2Y	3Y	4Y	5Y	7Y	10Y	14Y	20Y	30Y
Yield (Mean)	2.26	2.43	2.64	3.1	3.39	3.82	4.15	4.69	5.17	5.24
Yield (Standard Deviation)	1.73	1.64	1.48	1.37	1.24	1.32	1.31	1.13	1.13	1.22
Yield (Min)	0.08	0.15	0.02	0.07	0.43	0.72	1.02	0.85	2.29	2.51
Yield (Max)	8.68	18.1	11.16	7.64	8.08	9.38	9.39	12.34	9.71	9.8
No. of Unique CUSIPs	1359	1060	809	558	468	283	122	72	67	48
No. of Unique Issuers	173	159	149	112	108	81	57	41	39	37
No. of Daily Observations	5404	5086	4963	4817	4636	5270	4512	4112	4206	4376

(a) Prime and High Grade

	1Y	2Y	3Y	4Y	5Y	7Y	10Y	14Y	20Y	30Y
Yield (Mean)	2.55	2.74	3	3.35	3.46	4.04	4.37	4.98	5.27	5.31
Yield (Standard Deviation)	1.86	1.69	1.66	1.55	1.48	1.45	1.27	1.12	1.21	1.3
Yield (Min)	0.19	0.24	0.35	0.52	0.77	1.1	1.21	2.09	2.37	2.44
Yield (Max)	13.81	11.86	12.57	10.42	10.52	12.96	8.46	8.71	9.41	11.3
No. of Unique CUSIPs	2536	2226	1877	1407	1248	938	456	248	208	99
No. of Unique Issuers	395	361	339	274	252	227	161	117	116	68
No. of Daily Observations	5688	5688	5688	5688	5688	5688	5685	5618	5656	5133

(b) Upper Medium Grade

	1Y	2Y	3Y	4Y	5Y	7Y	10Y	14Y	20Y	30Y
Yield (Mean)	3.35	3.98	4.15	4.27	4.49	4.98	5.55	6.07	6.17	6.58
Yield (Standard Deviation)	2.24	3.1	2.59	1.93	2.05	1.58	1.49	1.22	1.27	1.25
Yield (Min)	0.33	0.53	0.82	0.73	1.07	1.76	1.94	2.52	3.19	2.48
Yield (Max)	30.62	30.57	27.26	20.66	25.63	17.17	15.56	12.6	12.51	16.08
No. of Unique CUSIPs	1444	1232	1032	800	666	664	414	312	236	117
No. of Unique Issuers	440	406	369	309	274	264	201	162	137	77
No. of Daily Observations	5680	5679	5665	5652	5639	5688	5645	5603	5407	5554

(c) Lower Medium Grade

Note: This table reports summary statistics for daily aggregate corporate bond yields by credit rating category and maturity. Yields are expressed in percent and are constructed following the procedure described in Section 3.1. Maturities range from 1 to 30 years; we additionally report 4-year and 14-year maturities to provide a more detailed characterization of the term structure, although these maturities do not correspond to standard Treasury issuance benchmarks. The sample spans 5,688 trading days from June 2002 to March 2025. The number of daily observations in each maturity-rating cell may be smaller than the total number of trading days because no bond in a given rating category and maturity bucket may trade on a particular day. "No. of Unique CUSIPs" and "No. of Unique Issuers" report the total number of distinct securities and issuing firms contributing to each maturity bucket over the sample period.

the Federal Reserve Bank of New York records indicative bid/ask quotes in the Treasury market. Consequently our daily data are constructed such that on the day of an FOMC announcement, the monetary policy shock will be predetermined with respect to both the Treasury yields and the

corporate bond yields recorded for that day. We then calculate the credit spread for each credit rating and maturity category by subtracting the Treasury yield from the aggregate corporate bond yield of the same maturity.[12]

However, instead of estimating our regressions at the daily frequency, we instead run them at the FOMC announcement frequency. That is, we calculate average Treasury yields and average credit spreads across days between the start of consecutive FOMC announcements. This is done for the following reasons. First, daily data suffers from a high degree of market microstructure noise that should, in principle, wash out in the aggregate when averaged over a longer time horizon. By aligning the frequency of our observations with the policy cycle, we effectively summarize the cumulative effects of a monetary policy shock between meetings and reduce transitory high-frequency noise, thereby yielding a potentially stronger signal-to-noise ratio. On the other hand, the noise may increase as more economic news and as well as more shocks to Treasury yields and credit spreads that do not pertain to monetary policy are realized within a longer time-frame. However, we have good reason to believe that this will be counter-balanced by a stronger signal, given the relative lack of liquidity in the corporate bond market compared to other asset classes. Investors in this market may take time - on the order of several days or weeks - to digest information released in an FOMC meeting, and portfolio rebalancing decisions that reflect this updated information may take time on the order of weeks and months. Similarly, balance-sheet frictions such as search costs faced by dealers may slow down the transmission of information in this market as inventories sluggishly adjust to changing investor demands based on this monetary policy shock. Moreover, as will be shown later in the paper, the systematic component of credit spreads is also highly persistent. Thus, averaging credit spreads between FOMC dates is more likely to capture the full

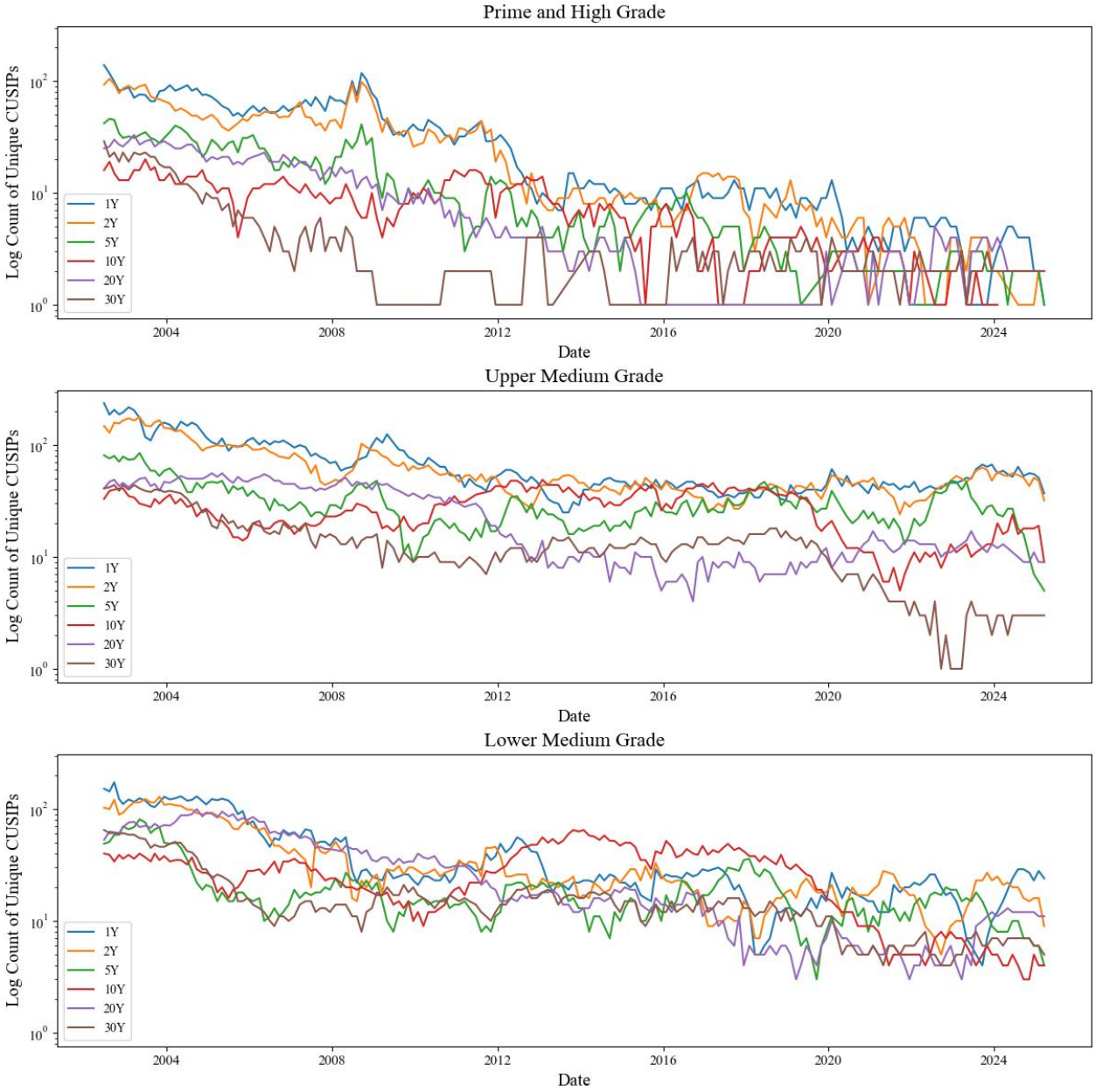
[12]In constructing spreads, we do not explicitly duration-match corporate and Treasury securities as is done in Gilchrist and Zakrajšek (2012). This simplification is unlikely to materially affect our results for several reasons. First, over 85% of bonds in our sample pay semi-annual coupons, consistent with the coupon frequency of Treasury securities, implying that systematic differences in duration arising from payment structure are limited. Second, we restrict attention to standard fixed-coupon ("vanilla") corporate bonds and exclude securities with embedded optionality or other complex contractual features that would generate substantial heterogeneity in effective duration. Third, we apply cross-sectional aggregation to attenuate idiosyncratic pricing noise and microstructure distortions at the bond level. Because spreads are computed at the credit-maturity group level rather than bond-by-bond, residual duration mismatches are further smoothed within each class. To the extent that any remaining mismatch persists, it is plausibly second-order relative to the cross-sectional and time-series variation in spreads induced by monetary policy shocks.

adjustment process to monetary policy shocks compared to measurements at the daily frequency.

Second, by aggregating at the FOMC announcement frequency, we face fewer issues with missing data and computed yields being unrepresentative of the credit rating and tenor category due to small sample counts. In Figure 1, we plot the number of unique issuances traded in each credit and maturity category within an FOMC period on a logarithmic scale. Compared to the eight-week moving average of the number of unique CUSIPs transacted daily in each credit and maturity category shown in Figure 5 in the Appendix, we observe that we have almost twice as high a sample count per period when we aggregate at the FOMC frequency level. This helps to mitigate partially the low observation counts that occur particularly for Prime and High Grade and Lower Medium Grade bonds of a longer tenor. Moreover, as Figure 6 in the Appendix demonstrates, these samples originate from a wide variety of issuers, and thus our aggregate credit spread measures are not solely driven by the characteristics of a few firms. That said, a noticeable decline in the sample count still remains especially for Prime and High Grade bonds. There are perhaps two contributing factors to this phenomenon. The first is that post-Global Financial Crisis, tightened rating standards have meant that fewer corporate bonds have been awarded triple-A or double-A status. The second is that the issuance of corporate bonds with embedded optionality has rapidly grown over the past two decades, and as noted previously these bonds have been excluded from our sample. The concern then is that the dynamics of Prime and High Grade bonds, and to a lesser extent Lower Medium Grade bonds, is driven by only a select few of bonds, particularly in the later half of our sample period when measured at the daily frequency. Aggregating daily data over a longer time interval helps partially to mitigate many of these issues of missing observations, while maintaining the representativeness of the sample.

Third, by defining the time between the start of consecutive FOMC announcements as our event time for the pooled observations, we match our trading frequency for bond yields with that for the observation frequency for monetary policy shocks. In this setting, we retain the timing structure whereby monetary policy shocks occur at the start of every period before the Treasury and corporate bond yields are measured. Shorter periods such as a week or a month face the

Figure 1: Trading Breadth by Credit Rating and Maturity



Note: The figure plots the time series of the number of unique CUSIPs traded within each FOMC intermeeting period, separately for Prime and High Grade (top panel), Upper Medium Grade (middle panel), and Lower Medium Grade (bottom panel) bonds. Within each panel, we report selected maturity buckets (1-, 2-, 5-, 10-, 20-, and 30-year). The vertical axis shows the logarithm of the count of unique CUSIPs. The vertical axis displays the natural logarithm of the number of unique CUSIPs traded. All panels share a common logarithmic scale to facilitate cross-category comparisons. The data are drawn from TRACE and span January 2002 through March 2025.

Table 2: Summary Statistics for Treasury Yields and Credit Spreads

	1Y	2Y	3Y	5Y	7Y	10Y	20Y	30Y
Yield (Mean)	1.81	1.96	2.13	2.50	2.80	3.08	3.60	3.70
Yield (Standard Deviation)	1.77	1.60	1.47	1.29	1.19	1.13	1.14	1.05
Yield (Min)	0.05	0.13	0.16	0.26	0.46	0.65	1.14	1.36
Yield (Max)	5.44	5.09	5.04	5.03	5.05	5.10	5.46	5.55
No. of Missing Observations	0	0	0	0	0	0	0	0

(a) Constant Maturity Treasury Yields

	1Y	2Y	3Y	5Y	7Y	10Y	20Y	30Y
Spread (Mean)	0.52	0.61	0.63	0.74	0.98	1.09	1.29	1.39
Spread (Standard Deviation)	0.63	0.58	0.38	0.74	0.78	0.56	0.38	0.70
Spread (Min)	-1.40	-0.29	-0.13	-1.67	-0.04	0.28	0.71	0.69
Spread (Max)	4.3	4.59	2.60	3.76	4.98	3.49	2.97	5.01
No. of Missing Observations	3	5	4	14	0	13	15	13

(b) Prime and High Grade

	1Y	2Y	3Y	5Y	7Y	10Y	20Y	30Y
Spread (Mean)	0.75	0.79	0.89	0.98	1.25	1.30	1.69	1.62
Spread (Standard Deviation)	0.93	0.81	0.90	0.81	0.94	0.67	0.58	0.79
Spread (Min)	0.02	0.13	0.19	0.32	0.49	0.38	0.87	0.58
Spread (Max)	7.01	5.95	6.64	5.62	6.47	4.79	4.18	5.93
No. of Missing Observations	0	0	0	0	0	0	0	0

(c) Upper Medium Grade

	1Y	2Y	3Y	5Y	7Y	10Y	20Y	30Y
Spread (Mean)	1.56	2.03	2.03	2.01	2.19	2.5	2.55	2.89
Spread (Standard Deviation)	1.61	2.67	2.24	1.68	1.25	1.06	0.79	0.94
Spread (Min)	0.42	0.62	0.70	0.68	0.98	0.93	1.45	1.64
Spread (Max)	9.44	19.48	15.8	12.72	9.11	8.72	6.33	8.14
No. of Missing Observations	0	0	0	0	0	0	0	0

(d) Lower Medium Grade

Note: This table reports summary statistics for U.S. constant maturity Treasury yields and corporate bond spreads measured at the Federal Open Market Committee (FOMC) announcement frequency. Observations correspond to periods between scheduled FOMC meetings (N = 182). Yields are expressed in percent at maturities of 1-, 2-, 3-, 5-, 7-, 10-, 20-, and 30-years. Corporate bond spreads are measured relative to maturity-matched Treasury yields and are reported in percentage points. "Prime and High Grade," "Upper Medium Grade," and "Lower Medium Grade" refer to rating-based corporate bond categories. The table reports the mean, standard deviation, minimum, maximum, and the number of missing observations for each series.

issue that missing data on the shock series between periods becomes more severe. Moreover, we would have to take significant care in configuring the start and end of each period to ensure that the FOMC announcement did not occur in the middle of the period. This is made more difficult

by the fact that there are eight FOMC announcements in a calendar year, and the number of days between meetings varies over time. While redefining a period in terms of the time between FOMC announcements introduces heteroskedasticity as mean yields are calculated across slightly varying sample lengths, we argue that this is a small price to pay given all the concerns described above. In addition, note that this time variation in sample lengths is unlikely to produce bias in our estimation since we focus on scheduled FOMC announcements, and so this variation is plausibly independent of the monetary policy shocks. Were we to include unscheduled FOMC announcements, we may be concerned that the fewer days between announcements were correlated with significant market disruptions, during which the volatility of monetary policy shocks was higher as a result of greater uncertainty surrounding policies proposed to address such an event.[13] With the Treasury bond yields and credit spreads aggregated at the FOMC meeting frequency, we are left with eight observations per period per credit rating category as summarized in Table 2.

In the following section, we describe how we use these data to estimate IRFs of credit spreads to monetary policy shocks. We achieve this through using local projections first and then relate the significance of our findings to the three hypotheses outlined in the earlier section.

3.2 Estimating Impulse Response Functions of Credit Spreads to Monetary Policy Shocks Using Local Projections

For robust identification of the causal response of credit spreads to a monetary policy shock, we use a variety of different measurements of the time series of monetary policy shocks available in the recent literature as our regressors of interest. The principal sources are Jarociński and Karadi (2020), Bauer and Swanson (2023b), and Acosta et al. (2025), which date from February 1990 to December 2025, February 1988 to December 2023, and February 1994 to January 2026 at the time of retrieval respectively. Common to all of these papers is the construction of the monetary policy shock using a variety of relevant asset prices recorded within a narrow window of the FOMC

[13] In short, our work is more akin to the spirit of a conventional event study with the difference that our event dates are known in advance and, hence, perfectly predictable. Thus, the timing of the monetary policy announcements is unlikely to confound the causal effects studied in this paper.

announcement and/or subsequent press conference. These studies follow in the footsteps of earlier work by Kuttner (2001), Gürkaynak et al. (2005), and Gertler and Karadi (2015). The asset prices used to construct these measures typically include some combination of short-rate instruments such as federal funds futures rates, eurodollar rates, and overnight index swap rates, and may also involve Treasury yields and S&P 500 index returns. Aggregation is then usually done through taking principal components of the panel of asset price changes. Meanwhile, the window of measurement is often between thirty minutes and two hours in length. This compromise reflects the tradeoff between a narrower window, which may fail capture the market's full response and reassessment to a monetary policy surprise, against a wider window, which risks the contamination of the market response with other sources of relevant pricing information that are unrelated to monetary policy.

To distinguish between the different measurements of monetary policy shock that we employ in the different regression specifications, we use the initials of the corresponding authors and creators of the measurement as superscript alongside a brief descriptor. They are as follows: $x_t^{JK,MPS}$ and $x_t^{JK,CBI}$ to denote the pure monetary policy component and the central bank information component in Jarociński and Karadi (2020), $x_t^{BS,ORIG}$ and $x_t^{BS,ORTH}$ to denote the unorthogonalized and the orthogonalized measurements with respect to public macroeconomic data in Bauer and Swanson (2023b), and $x_t^{AABLMA,S}$ for measurements around the FOMC statement only and $x_t^{AABLMA,P}$ for measurements around the FOMC press conference as measured by Acosta et al. (2025). To ensure that the regression coefficients on each measure of the monetary policy shock are comparable, we first standardize them to have zero mean and a standard deviation of one before using them in the local projection.

For our dependent variable, we have credit spreads y of some credit rating i, where i is either Lower Medium Grade, Upper Medium Grade, or Prime and High Grade. For convenience, we use a one-hot encoding such that these correspond to 0, 1, and 2, respectively. For the credit spread maturities, we have eight in total. Instead of encoding all eight maturities, we instead offer a simpler alternative that will later be conducive to testing for monotonicity. We let maturity j to be short-term (0), medium-term (1), or long-term (2) respectively. To compute these corresponding spreads,

Table 3: Average Contemporaneous Response of Credit Spreads Across Five Specifications

	(1)	(2)	(3)	(4)	(5)
const	0.319	1.384**	0.539	1.940**	1.634
	(0.792)	(0.567)	(0.663)	(0.895)	(2.723)
$x_t^{JK,MPS}$	0.071*	0.117**	0.105***	0.133***	0.151***
	(0.038)	(0.045)	(0.027)	(0.032)	(0.035)
Observations	1109	997	920	857	795
R^2	0.485	0.514	0.537	0.552	0.565

Note: All regressions include lagged yields and spreads ($W_{t-1:t-1-p}$) as controls; coefficients on these lagged terms are omitted for brevity. The reported coefficient on $x_t^{JK,MPS}$ captures the contemporaneous effect of the unanticipated monetary policy shock following Jarociński and Karadi (2020). Column headers indicate the number of lags p included in each specification. Driscoll-Kraay standard errors robust to heteroskedasticity and cross-sectional dependence are reported in parentheses. Significance levels: ***p<0.01, **p<0.05, *p<0.1.

we define short-term to be the mean of the 1-year and 2-year spread, medium-term to be the mean of the 3-year, 5-year, and 7-year spread, and long-term to be the mean of the 10-year, 20-year, and 30-year. We further require that all spreads used in the calculation of the mean for that credit rating and period in time be available. Otherwise, the mean is treated as missing data. This ensures that all of the spreads are roughly centered on the same maturity date for each group $j=0,1,2$.

Although our monetary policy shocks are assumed to be exogenous, for efficiency purposes, we additionally control for the yields and spreads observed in prior periods, which we summarize as the matrix of covariates $W_{t-1:t-1-p}$ up to some lag p. To begin, let us consider the average contemporaneous treatment effect of monetary policy shocks on credit spreads across the entire sample:

$$y_t = \alpha + \beta x_t^{JK,MPS} + \gamma' W_{t-1:t-1-p} + \epsilon_{i,j,t}, \tag{15}$$

where our regressor of interest is the pure monetary policy shock as defined in Jarociński and Karadi (2020), $x_t^{JK,MPS}$. This shock is constructed under the assumption that the unanticipated component of monetary policy causes higher interest rates and lower stock market prices on impact, as opposed to the systematic or informational component which causes higher interest rates and higher stock prices on impact. $x_t^{JK,MPS}$ is the output from the median rotation of the principal components of changes in short-term interest rates such that this negative sign restriction

is satisfied. Consequently, this shock is perhaps closest in nature to the Brownian motion on the short rate process in our theoretical model when ρ is assumed to be negative.

Table 3 reports the estimates of the contemporaneous effect of an unanticipated monetary policy shock, $x_t^{JK,MPS}$, on credit spreads across five specifications. Each column progressively includes additional lags of yields and spreads ($W_{t-1:t-1-p}$) as controls. Positive coefficients indicate a widening of credit spreads. Across all specifications, the estimated effect is positive and economically meaningful, ranging from a 7-basis-point (bp) increase to a 15-bp increase in response to a one-standard-deviation shock. In Column 1, which includes only the shortest lag of yields and spreads, the effect is 0.071 and significant at the 10% level. As additional lags are included (Columns 2–5), the magnitude increases monotonically, reaching 0.151 in Column 5, significant at the 1% level. This pattern suggests that controlling for lagged yields and spreads helps isolate the effect of unanticipated policy changes and highlights the robustness of the response. In particular, the increase in R^2, from 0.485 to 0.565, illustrates that credit spreads are persistent and that controlling for their lagged values reduces residual variance and partially enhances the precision of estimation.

For comparison, Table 4 reports the estimated contemporaneous effects of an unanticipated monetary policy shock, $x_t^{JK,MPS}$, on Treasury yields across short-, medium-, and long-maturity segments. These are the results from running the regression in Equation 15, with y_t being the time series of average Treasury yields for one of the three maturity segments, the controls, $W_{t-1:t-1-p}$, consisting solely of lagged Treasury yields, and the lag length $p=3$ being chosen to minimize the AIC and BIC on top of an additional lag included to improve finite-sample inference following Montiel Olea and Plagborg-Møller (2021).

As expected, the estimated contemporaneous effect of an unanticipated monetary policy shock, $x_t^{JK,MPS}$, is positive across all maturities, indicating that contractionary shocks raise yields along the curve. Short-term yields (s) increase modestly by 3.6 bps, while medium- and long-term yields (m and l) respond slightly more strongly, at 5.3 and 4.9 bps, respectively, both significant at the 5% level. This maturity pattern reflects the forward-looking nature of long-term rates, which gradually incorporate unexpected policy moves.

Table 4: Average Contemporaneous Treatment Effects Across the Treasury Yield Curve

	(Short Maturity)	(Medium Maturity)	(Long Maturity)
const	0.100*	0.100	0.101
	(0.060)	(0.073)	(0.068)
$x_t^{JK,MPS}$	0.036	0.053**	0.049**
	(0.022)	(0.025)	(0.025)
y_{t-1}^s	1.659***	0.421	0.234
	(0.230)	(0.263)	(0.237)
y_{t-1}^m	-0.237	0.824**	-0.152
	(0.243)	(0.325)	(0.366)
y_{t-1}^l	0.055	0.121	1.178***
	(0.169)	(0.222)	(0.274)
Observations	178	178	178
R^2	0.985	0.963	0.954

Note: All specifications include lagged yields up to three lags, $W_{t-1:t-1-p}$, as controls; coefficients on these lagged terms following the first lag are omitted for brevity. The lag length $p=3$ is selected by minimizing the AIC and BIC, with one additional lag included to improve finite-sample inference following Montiel Olea and Plagborg-Møller (2021). The reported coefficient on $x_t^{JK,MPS}$ captures the contemporaneous effect of the unanticipated monetary policy shock identified in Jarociński and Karadi (2020). Treasury yields averaged over maturity groupings are constructed from constant-maturity yields obtained from FRED. Superscripts denote maturity groupings: s (short) is the average of the one- and two-year yields; m (medium) is the average of the three-, five-, and seven-year yields; and l (long) is the average of the ten-, twenty-, and thirty-year yields. Heteroskedasticity-robust (HC3) standard errors are reported in parentheses. Significance levels: *** $p<0.01$, ** $p<0.05$, * $p<0.10$.

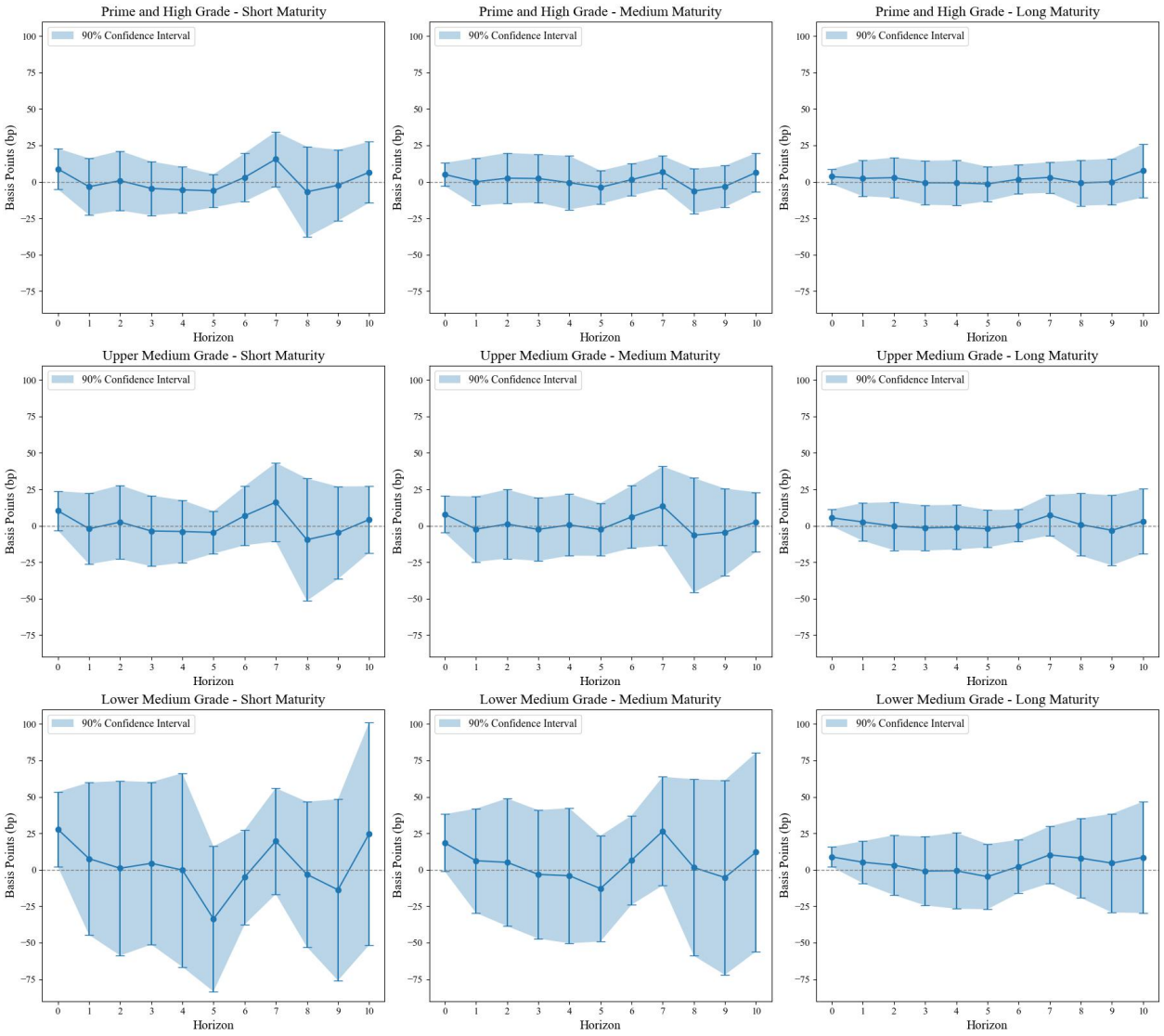
Comparing these results with the effects on credit spreads reported in Table 3, we observe that credit spreads respond more strongly to the same unanticipated monetary policy shock. On average, a one-standard-deviation monetary policy shock increases credit spreads by more than 10 bps, whereas the average contemporaneous effect on Treasury yields across maturities is approximately 5 bps. This implies that the transmission of monetary policy through a risk premium channel to credit spreads is quantitatively more pronounced than through a pure term-structure channel to Treasury yields, even though both channels respond consistently to policy surprises.

Next, let us consider the dynamic effects of an unanticipated monetary policy shock on credit spreads across different credit ratings and maturities. To do this, we run the following local projection at horizons h from 0 to 10:

$$y_{i,j,t+h} = \alpha_{i,j,h} + \beta_{i,j,h} x_t^{JK,MPS} + \gamma_{i,j,h}' W_{t-1:t-1-p} + \epsilon_{i,j,t+h}. \tag{16}$$

Figure 2 displays a three-by-three grid of the IRFs from running the local projection described

Figure 2: Local Projections of Various Aggregate Credit Spreads to a Monetary Policy Shock



Note: This figure reports impulse response functions estimated using the local projection method in Equation 16. Each panel corresponds to a different credit rating category (Prime and High Grade, Upper Medium Grade, and Lower Medium Grade) and maturity segment (short, medium, and long). The horizontal axis denotes the forecast horizon (in FOMC periods), and the vertical axis measures responses in basis points. Shaded areas represent 90% confidence intervals constructed from heteroskedasticity-consistent (HC3) standard errors.

in Equation 16 on the different aggregate credit spreads. The full table of coefficients and standard errors are presented in Table 8 in the Appendix. A primary observation is the monotonic increase in the contemporaneous response ($h = 0$) as credit quality deteriorates. For the Prime and High Grade cohorts (top row), the initial impact is statistically negligible, suggesting a degree of insulation where high-grade debt maintains its role as a stable store of value. Conversely, as we

migrate toward Lower Medium Grade issuers (bottom row), the instantaneous spread widening becomes more pronounced. This gradient reflects an amplification mechanism in line with our theoretical model: lower-tier (more risky) issuers have a more volatile assets, making their spreads more sensitive to monetary policy shocks.

The results further highlight an interaction between maturity and shock transmission. The Short Maturity column (extreme left) exhibits the highest degree of volatility and peak response magnitudes. This sensitivity in the short-end of the curve likely reflects heightened concerns regarding rollover risk and immediate liquidity constraints that become exacerbated under tighter monetary conditions. In contrast, Long Maturity issuances (extreme right column) display smoother, more attenuated impulse responses. While long-term instruments are subject to greater duration risk, their credit spreads appear better anchored. This is again in-line with our theoretical model, but it may also be potentially due to the market pricing in long-run solvency rather than transient market frictions.

Moreover, the visualization reveals a clear relationship between asset risk and estimation uncertainty. While the point estimates for lower-quality and shorter-maturity debt are larger in magnitude, they are accompanied by a substantial expansion of the 90% confidence intervals. This heteroscedasticity suggests that the idiosyncratic noise or market fragmentation within the Lower Medium Grade segment reduces the precision of the local projection. Consequently, while the central tendencies suggest a monotonic relationship between risk and response, the overlapping confidence intervals across rows indicate that a formal hypothesis test is required to confirm the statistical significance of this perceived monotonicity.

To address this concern, we additionally run a pooled regression, in which we further specify the following dummies $I(i \geq 1)$, $I(i \geq 2)$, $I(j \geq 1)$, and $I(j \geq 2)$. Our pooled regression is expressed

below:[14]

$$y_{i,j,t} = const + \beta x_t + \sum_{k=1}^{2} \beta_{k,\cdot} x_t I(i \geq k) + \sum_{l=1}^{2} \beta_{\cdot,l} x_t I(i \geq 1) + \sum_{k=1}^{2} \sum_{l=1}^{2} \beta_{k,l} x_t I(i \geq k) I(j \geq l) + \gamma' W_{t-1:t-1-p} + \epsilon_{i,j,t} \tag{17}$$

Observe that we have defined the dummies in such a way that the test for monotonicity becomes a one-sided test that the coefficient on that interaction is non-positive (although it is worth noting that statistical significance here is derived from a univariate test, not a joint test). In particular, given our model, we should expect all the coefficients on the (single) interaction terms to be negative. Inference on these coefficients, however, is complicated by the four significant features of our data. First, there is the potential for serial correlation within units if lag length p is insufficient. Second, there is considerable cross-sectional dependence across units at any given time. Third, as noted previously, since we take the average over varying sample lengths to construct our spreads for each FOMC period, the residuals in our pooled regression will most certainly exhibit heteroskedasticity. Fourth, to reiterate, our panel is unbalanced. To address these concerns, rather than perform two-way clustering as we only have nine units at most per time period, we instead adopt Driscoll-Kraay (DK) standard errors, which provide robust handling of serial and cross-sectional dependence under large T asymptotics (1998).

Table 5 below displays the results of the local projections for horizon $h=0$ and lag length $p=3$. We run these local projection across various monetary policy shocks and observe the following patterns in the contemporaneous response of credit spreads. First, across both specifications of the Bauer-Swanson shocks, a one standard-deviation shock induces an approximately 25-bp increase in the baseline credit spread corresponding to the response of Lower Medium, short maturity credit, consistent with a negative correlation between asset value innovations and the short rate. Single-dummy interactions are generally negative, indicating that higher-rated or longer-maturity credits

[14]Thus, for each period, we have a set of twelve controls consisting of short-term, medium-term, and long-term yields and spreads of Treasuries, Prime and High Grade credit, Upper Medium Grade credit, and Lower Medium Grade credit respectively, which are then further interacted with the dummy variables outlined above.

Table 5: Heterogeneous Contemporaneous Responses of Credit Spreads to Monetary Policy Shocks Across Ratings and Maturities

	Credit Spread $y_{i,j,t}$ for Rating i and Maturity j					
	BS,ORIG	*BS,ORTH*	*AABLMA,S*	*AABLMA,P*	*JK,MPS*	*JK,CBI*
x_t	0.2408**	0.2559**	0.2438**	0.2696**	0.2690***	-0.0297
	(0.1132)	(0.1080)	(0.1052)	(0.1199)	(0.0890)	(0.1153)
$x_t I(i \geq 1)$	-0.1449*	-0.1520*	-0.1422*	-0.1585*	-0.1699**	0.0388
	(0.0842)	(0.0779)	(0.0782)	(0.0889)	(0.0712)	(0.0721)
$x_t I(i \geq 2)$	-0.0269	-0.0332*	-0.0234	-0.0239	-0.0145	-0.0256
	(0.0173)	(0.0177)	(0.0174)	(0.0185)	(0.0191)	(0.0255)
$x_t I(j \geq 1)$	-0.0869	-0.0849	-0.0799	-0.0938	-0.0925	0.0051
	(0.0739)	(0.0692)	(0.0709)	(0.0799)	(0.0773)	(0.0555)
$x_t I(j \geq 2)$	-0.0793*	-0.0827*	-0.0883*	-0.0951*	-0.0925**	0.0161
	(0.0438)	(0.0420)	(0.0457)	(0.0494)	(0.0427)	(0.0565)
$x_t I(i \geq 1) I(j \geq 1)$	0.0726	0.0748	0.0645	0.0780	0.0699	0.0124
	(0.0710)	(0.0644)	(0.0689)	(0.0770)	(0.0761)	(0.0508)
$x_t I(i \geq 1) I(j \geq 2)$	0.0397	0.0399	0.0420	0.0437	0.0679**	-0.0633
	(0.0276)	(0.0261)	(0.0273)	(0.0298)	(0.0304)	(0.0486)
$x_t I(i \geq 2) I(j \geq 1)$	-0.0237	-0.0140	-0.0336	-0.0427	-0.0134	-0.0422
	(0.0259)	(0.0229)	(0.0276)	(0.0310)	(0.0287)	(0.0284)
$x_t I(i \geq 2) I(j \geq 2)$	0.0253	0.0227	0.0345	0.0392	0.0106	0.0475**
	(0.0256)	(0.0222)	(0.0263)	(0.0287)	(0.0233)	(0.0217)
Observations	920	920	920	920	920	920
R^2	0.964	0.966	0.965	0.964	0.965	0.960

Note: All specifications include lagged yields up to three lags, $W_{t-1:t-1-p}$, as controls; coefficients on these lagged terms following the first lag are omitted for brevity. The lag length $p=3$ is selected by minimizing the AIC and BIC, with one additional lag included to improve finite-sample inference following Montiel Olea and Plagborg-Møller (2021). The reported coefficient on $x_t^{JK,MPS}$ captures the contemporaneous effect of the unanticipated monetary policy shock identified in Jarociński and Karadi (2020). Treasury yields averaged over maturity groupings are constructed from constant-maturity yields obtained from FRED. Superscripts denote maturity groupings: s (short) is the average of the one- and two-year yields; m (medium) is the average of the three-, five-, and seven-year yields; and l (long) is the average of the ten-, twenty-, and thirty-year yields. Heteroskedasticity-robust (HC3) standard errors are reported in parentheses. Significance levels: *** $p<0.01$, ** $p<0.05$, * $p<0.10$.

experience smaller widening of spreads. Cross-interaction terms are broadly insignificant, with larger standard errors reflecting the smaller sample for these interactions. Orthogonalizing the shock to past and current macroeconomic data ($x_t^{BS,ORTH}$) has little effect on the estimated responses, suggesting that the informational content in monetary policy shocks is comparatively small. This is generally consistent with the findings of Bauer and Swanson (2023b) that orthogonalization of the shock matters less for correct inference when the dependent variable is an asset price.

Second, both the meeting-based ($x_t^{AABLMA,S}$) and statement-based ($x_t^{AABLMA,P}$) shocks produce positive baseline responses of roughly 24–27 basis points. Single-dummy interactions are negative, again indicating smaller effects for higher-rated or longer-maturity credit. Cross-interactions remain largely insignificant. As expected, the meeting-based shock, measured over a wider window and capturing larger monetary policy variation, produces somewhat larger coefficient magnitudes than the statement-based shock, consistent with its design to encompass more policy surprises.

Third, the pure monetary policy shock ($x_t^{JK,MPS}$) generates a positive and highly significant baseline effect (27 bp), consistent with the effects from the other shock measures. By contrast, the informational component ($x_t^{JK,CBI}$) demonstrates weak evidence of credit spreads narrowing following this shock, although the effect is not statistically significant. As discussed previously, this measure is constructed such that the monetary policy shock is positively correlated with stock market returns. This positive correlation implies that, on impact, the informational shock reflects anticipated policy responses to favorable economic news, which may increase asset values. As a result, credit spreads narrow to reflect higher corporate bond yield prices. Despite the modest magnitude of the response, this remains favorable evidence for the prediction that the magnitude and sign of the impulse response for credit spreads crucially depends on how the monetary policy shock correlates with the value of the firm. We rationalize this finding alongside the results for the Bauer-Swanson shocks by concluding that the informational component, while distinct in effect from the pure, unanticipated shock, is a much weaker signal, compared to the latter.

Overall, the evidence across all monetary policy shock series, with the exception of $x_t^{JK,CBI}$, indicates that: (i) baseline credit spreads increase significantly by approximately 25 bps in response to a one-standard-deviation monetary policy shock; (ii) longer-maturity credit exhibits attenuated responses, with consecutively longer segments widening roughly 8 bps less than shorter maturities; (iii) higher-rated credit experiences more muted responses, with the differential between Upper Medium and Lower Medium Grade (15 bps) being more pronounced than that between Prime/High Grade and Upper Medium Grade (3 bps); and (iv) coefficients on cross-interaction terms are generally statistically insignificant. Furthermore, orthogonalization or the explicit removal of the informational

components leads to only marginal gains in isolating the causal effect of the pure monetary policy shock. Finally, shocks constructed over broader windows (e.g., meeting-based series) tend to produce larger estimated effects, consistent with their design to capture greater monetary policy variation.

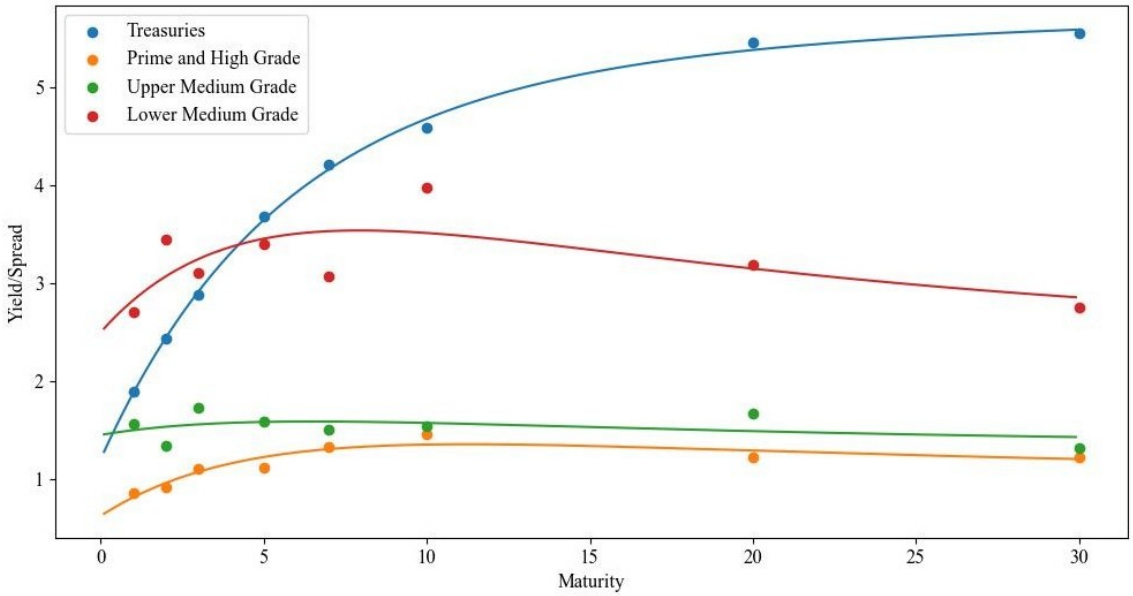
There are, however, several limitations to this exercise. While the regressions exhibit a high goodness of fit, standard errors remain substantial, suggesting that, despite soaking up excess variation, significant noise persists in the measurement of the underlying data. Large standard errors are also exacerbated by missing data, which is compounded when estimating pooled regressions with multiple lags, resulting in far fewer effective observations than a balanced panel would allow. Addressing this concern with missing data is therefore critical to improving efficiency. An alternative therefore is to use the full dataset rather than aggregating into three maturity categories. While this approach reintroduces idiosyncratic noise from individual maturities, it preserves information across the entire term structure, avoiding overly coarse aggregation. In the following section, we propose an estimation approach that addresses these issues: it handles missing data effectively and leverages the factor structure in the cross-section of credit spreads to improve efficiency.

4 A Nelson-Siegel State-Space Model of Credit Spreads and Monetary Policy Shocks

4.1 The Term Structure of Credit Spreads and Treasury Yields

A primary empirical challenge in our analysis is the significant idiosyncratic noise present in the corporate bond data, even after exhaustive cleaning and aggregation. As illustrated by the dispersion of individual observations in Figure 3, the processed data exhibit substantial variation, particularly within the lower-rated segments. In contrast, the Treasury yield curve demonstrates a significantly tighter fit to the interpolated cross-section, reflecting the deeper liquidity and structural stability inherent in sovereign debt markets. Our interpolation reveals that while the Treasury curve maintains a conventional, monotonically increasing profile consistent with a positive

Figure 3: Treasury Yield and Credit Spread Curve Estimates



Note: This figure illustrates the term structure of interest rates and credit spreads, depicting time-series averages of daily yields and spreads calculated over the inter-meeting window between the fourth and fifth Federal Open Market Committee (FOMC) meetings of 2002 (June 26 to August 13). The scatter points represent these period-averaged market observations for U.S. Treasuries and select credit rating cohorts. The empirical curves are estimated by fitting the parsimonious Nelson-Siegel framework (1987) to the averaged data, where the exponential decay parameter is held constant at $\lambda = 0.2$ across all asset classes.

duration risk premium, the credit spread curves display a distinct non-monotonic, "hump-shaped" geometry in line with prior empirical studies of the risk structure of credit (Sarig and Warga, 1989). This curvature is most acute in the Lower Medium Grade cohort, where spreads peak at the intermediate seven-to-ten-year horizon before exhibiting compression at the long end of the tenor structure. This concave term structure suggests that marginal default risk is concentrated in the intermediate maturities, potentially reflecting market-implied mean reversion in firm-level credit quality or the survival bias typically associated with long-dated corporate debt. Furthermore, the vertical displacement between cohorts highlights a substantial risk premium jump between Upper Medium and Lower Medium categories, particularly at the ten-year maturity. Conversely, the spreads for Prime and Upper Medium Grade issuers remain relatively compressed and flat, indicating that credit risk for high-quality signatures was perceived as largely maturity-invariant. This evidence complements our prior findings that the heterogeneity in responses to monetary policy shocks is more pronounced across lower-tier credit ratings than among high-grade signatures. As

Table 6: Cumulative Variance Explained by Principal Components of the Term Structure

	PC1	PC2	PC3	PC4	PC5
Treasuries	0.880	0.994	0.999	0.999	1.000
Prime and High Grade	0.771	0.852	0.915	0.951	0.972
Upper Medium Grade	0.914	0.958	0.974	0.984	0.990
Lower Medium Grade	0.894	0.930	0.959	0.976	0.988

Note: This table reports the cumulative proportions of variance explained by the first five principal components (PCs) for U.S. Treasury yields and credit spreads across rating cohorts. The sample period spans June 2002 to March 2025. Due to varying data availability, the PCA for Treasuries, Upper Medium Grade, and Lower Medium Grade is based on $N = 182$ observations, while the Prime and High Grade cohort is restricted to $N = 125$.

demonstrated by the historical time series in Figure 7 in the Appendix, these cross-sectional patterns are persistent features of the data throughout our sample period rather than transitory artifacts.

To fit the Treasury yield curve and credit spread curve in Figure 3, we smooth the period-averaged scatter observations using the three-factor Nelson-Siegel framework (1987). To motivate this choice of model, we first confirm that the term structure of credit spreads similarly admits a sparse factor representation much like the term structure of Treasury yields. Table 6 tabulates the cumulative variance explained by the first five principal components of Treasury yields, Prime and High Grade credit spreads, Upper Medium Grade credit spreads, and Lower Medium Grade credit spreads respectively. Where data is missing, the time period is dropped from the sample. As is well-documented in the literature, the first three principal components capture almost all of the variation in Treasury yields. Somewhat surprisingly, the first three principal components additionally account for between 90% and 98% of the variation of credit spreads across the three credit rating categories.

Moreover, as Table 7 demonstrates, the empirical maturity loadings of the extracted principal components exhibit a strong structural alignment with the level and slope factors characterized in the Nelson-Siegel model. Specifically, the first principal component (PC1) displays near-uniform factor loadings across the term structure for all three credit rating cohorts, a feature most prominent in the Upper Medium Grade spreads, which is consistent with a parallel shift or "level" factor. Conversely, the loadings on the second principal component (PC2) exhibit a monotonic increase across the maturity spectrum, analogous to the "slope" or "tilt" factor. While a perfect correspondence is not expected - given that principal components are orthogonal by construction, whereas

Table 7: Principal Component Factor Loadings across the Maturity Spectrum

(a) First Principal Component (PC1: Level Factor)

	1Y	2Y	3Y	5Y	7Y	10Y	20Y	30Y
Treasuries	0.463	0.431	0.404	0.359	0.323	0.291	0.263	0.224
Prime and High Grade	0.368	0.342	0.160	0.408	0.488	0.329	0.187	0.418
Upper Medium Grade	0.412	0.362	0.395	0.361	0.418	0.288	0.222	0.325
Lower Medium Grade	0.353	0.592	0.489	0.358	0.272	0.187	0.155	0.160

(b) Second Principal Component (PC2: Slope Factor)

	1Y	2Y	3Y	5Y	7Y	10Y	20Y	30Y
Treasuries	-0.457	-0.317	-0.185	0.050	0.198	0.331	0.491	0.514
Prime and High Grade	-0.521	-0.488	-0.222	0.559	0.005	0.128	-0.081	0.326
Upper Medium Grade	-0.349	-0.246	-0.352	-0.148	0.106	0.324	0.527	0.527
Lower Medium Grade	-0.150	-0.421	-0.114	0.120	0.273	0.600	0.361	0.456

(c) Third Principal Component (PC3: Curvature Factor)

	1Y	2Y	3Y	5Y	7Y	10Y	20Y	30Y
Treasuries	0.591	-0.000	-0.327	-0.454	-0.349	-0.066	0.262	0.379
Prime and High Grade	0.031	0.228	0.317	0.651	-0.456	-0.095	0.147	-0.429
Upper Medium Grade	-0.043	0.010	0.117	0.001	-0.217	-0.285	-0.503	0.776
Lower Medium Grade	-0.018	-0.309	0.728	-0.498	0.084	0.215	-0.060	-0.262

Note: This table reports the eigenvectors (loadings) associated with the first three principal components of the term structure of Treasury yields and credit spreads. The sample period spans June 2002 to March 2025. Consistent with the literature, the first three components are interpreted as Level, Slope, and Curvature factors, respectively. For Treasuries, Upper Medium Grade, and Lower Medium Grade, the sample consists of $N = 182$ observations, while the Prime and High Grade cohort is based on $N = 125$ observations due to data availability constraints. Loadings represent the sensitivity of each maturity tenor to a one-standard-deviation innovation in the respective factor.

Nelson-Siegel factors do not impose such a restricted covariance structure - the results confirm that a low-dimensional factor representation effectively captures the predominant cross-sectional variation in credit spreads. Furthermore, these findings suggest that dimension reduction serves as a robust filter for idiosyncratic noise, preserving the underlying term structure while enhancing the signal-to-noise ratio in credit spread data.

Consequently, we propose an alternative empirical specification to refine the estimation of IRFs characterizing the transmission of monetary policy shocks to the term structure of credit

spreads. Let $y_{i,\tau,t}$ denote an observed Treasury yield or credit spread i of maturity τ at time t, and let x_t^{MP} represent the monetary policy shock. In previous specifications, including the full vector of observed yields and spreads as controls was avoided to mitigate severe multi-collinearity and the subsequent loss of degrees of freedom. While coarse aggregation - such as averaging yields across maturity buckets - offers a preliminary solution, it discards valuable information regarding the term structure. A more principled approach recognizes that the term structures of both risk-free and credit-risky instruments are parsimoniously captured by low-dimensional factor models. If the factors, f_t, were directly observable, we could preserve the information content of the entire term structure while maintaining a tractable estimation framework:

$$y_{i,\tau,t+h} = \alpha_{i,\tau,h} + \beta_{i,\tau,h} x_t^{MP} + \sum_{l=1}^{p} \delta'_{i,\tau,h,l} f_{t-l} + \epsilon_{i,\tau,h,t}. \tag{18}$$

In this specification, the IRFs of interest are identified by the coefficient sequence $\{\beta_{i,\tau,h}\}_{h\geq 0}$. However, because f_t is latent, the local projection expressed in Equation 18 is not directly feasible. One potential resolution is a two-step procedure whereby inference of the factors is performed first through imposing a functional form on the factor loadings c:

$$y_{i,\tau,t} = \mu_{i,\tau} + c'_{i,\tau} f_t + u_{i,\tau,t}. \tag{19}$$

Following evidence in the previous section that the principal components of credit spreads align with the level, slope, and curvature factors, we may choose to specify the loadings in line with the Nelson-Siegel framework:

$$\begin{aligned} c_1(\tau) &= 1, \\ c_2(\tau) &= \frac{1-e^{-\tau\lambda}}{\tau\lambda}, \\ c_3(\tau) &= \frac{1-e^{-\tau\lambda}}{\tau\lambda} - e^{-\tau\lambda}, \end{aligned} \tag{20}$$

where the slope and curvature loadings c_2 and c_3, are governed by the exponential decay λ. By

estimating a series of cross-sectional regressions, we can extract the latent factors while filtering out idiosyncratic noise. The resulting measurement residual, $u_{i,\tau,t}$, accounts for localized liquidity effects and measurement error. Crucially, valid causal inference in this context requires that $u_{i,\tau,t}$ be orthogonal to the policy shock x_t^{MP}, ensuring the extracted factors capture the exhaustive systematic channels of policy transmission. If x_t^{MP} were correlated with the measurement residuals $u_{i,\tau,t}$, the resulting estimates would suffer from omitted variable bias, as the model would fail to distinguish between policy transmission and localized market idiosyncratic shocks.

Despite the intuitive appeal of this two-step approach, treating inferred factors as observed data introduces a generated regressors problem. This can lead to biased standard errors, undermining the reliability of the estimated dynamic causal effects. To overcome these limitations, we reformulate the system into the linear state-space model expressed in Equation 21, permitting joint estimation of the state transition and observation equations via the Kalman Filter. By redefining the latent factor vector, we cast the state transition into a VAR(1) process in companion form - a representation consistent with standard Gaussian affine term-structure models. To our knowledge, this study is the first to leverage such a framework specifically for structural causal inference in a monetary policy context.

$$\begin{aligned} F_t &= \mu_F + A(F_{t-1} - \mu_F) + e_t, \quad e_t \sim \text{wn}(B), \\ Y_t &= \mu_Y + CF_t + u_t, \quad u_t \sim \text{wn}(D). \end{aligned} \tag{21}$$

A key methodological departure from the extant term structure literature is our decision to forgo the formal imposition of no-arbitrage restrictions during the estimation procedure. It is important to note, however, that in a restricted case where the observation vector Y_t consists solely of zero-coupon Treasury yields, our econometric specification nests the arbitrage-free dynamic Nelson-Siegel (AFDNS) model of Christensen et al. (2011). In that context, the no-arbitrage condition imposes a specific cross-sectional restriction on the intercept term μ_Y; we relax this constraint to facilitate a more tractable estimation without compromising the structural integrity of the resulting IRFs. Our choice to prioritize flexibility over formal no-arbitrage constraints is further motivated by the findings of Joslin et al. (2013), who demonstrate that such restrictions often provide negligible

improvements in the estimation of term structure dynamics and impulse response functions.

This state-space approach offers the distinct advantage of facilitating a joint estimation across the entire cross-section of yields and spreads, rather than requiring separate multi-stage regressions for each rating cohort and maturity. By pooling the four term structures — each characterized by a three-factor representation — and augmenting the system with a state variable for the monetary policy shock that is ordered first in the VAR, we obtain a comprehensive latent factor vector of dimension $K=13$. Incorporating $p=3$ lags to account for transition dynamics, the resulting state vector in companion form, F_t, has a dimension of $Kp=39$. The observation vector Y_t comprises of $N=36$ elements, representing 11 Treasury yield maturities and 8 credit spread maturities for each of the three credit rating classes. Within this framework, A denotes the $Kp \times Kp$ transition matrix, while C represents the $N \times Kp$ factor-loading matrix, where each row following the first row is populated by the corresponding Nelson-Siegel loadings for its respective maturity and asset class.[15] The stochastic structure is governed by the covariance matrices B and D for the transition and observation equations, respectively. By construction, we impose the restriction that innovations in the state transition equation are orthogonal to the measurement errors in the observation equation. This assumption nests our previous requirement that the monetary policy surprise is exogenous with respect to idiosyncratic noise and liquidity-driven fluctuations in both Treasury yields and credit spreads, thereby ensuring the estimated IRFs have a causal interpretation.

In addition, the model as currently formulated requires further restrictions before structural identification of the parameters can be achieved. First, the intercept terms μ_F and μ_Y are not separately identified due to the standard level-shift indeterminacy in linear models. We therefore normalize the observation intercept to zero, $\mu_Y = \mathbf{0}$, in line with the fact that we have standardized the monetary policy shock beforehand. Second, the loading matrix C is generally subject to rotational indeterminacy in latent factor frameworks. In the subsequent section, we establish the sufficient rank and

[15] Note that under the convention where the first element of the observation vector Y_t is also the shock x_t^{MP}, the corresponding loading is given by $C_{1,1}=1$ and $C_{1,j}=0$ for $j \neq 1$. Crucially, we impose a structural exclusion restriction on the remainder of the observation equation such that all other yields and spreads do not load directly on the policy factor ($C_{j,1}=0$ for $j>1$). Thus, the impact of a monetary policy shock on the term structures propagates endogenously via its influence on the latent pricing factors.

order conditions for the identification of C and demonstrate that the Nelson-Siegel parametrization satisfies these criteria by imposing a fixed functional form on the cross-sectional loadings.

Third, the model as currently specified is in reduced form, as the innovations in the state transition equation do not yet represent structural economic shocks. Analogous to reduced-form vector autoregressions, these innovations are identified only up to an orthogonal rotation. However, given that our monetary policy shock is predetermined with respect to the yields and spreads within the same period, we can identify the structural innovations via a Cholesky decomposition of the state covariance matrix B when the monetary policy shock is ordered first. Given the latent nature of this vector autoregression, we call this identification strategy *Latent SVAR*. As formally proven in the following section, the joint identification of the transition matrix A, the loading matrix C, and the lower-triangular Cholesky factor of B is sufficient to uniquely reconstruct the IRFs characterizing the transmission of monetary policy shocks to the term structures of interest rates and credit spreads.

4.2 Estimating Impulse Response Functions of Credit Spreads to Monetary Policy Shocks Using Latent SVAR

Let us first consider the general latent factor representation. Let the state vector $\{F_t\}_{t\geq 1}$ and the observation vector $\{Y_t\}_{t\geq 1}$ be governed by the following linear state-transition and measurement equations:

$$\begin{aligned} F_t &= AF_{t-1} + e_t, \quad e_t \sim \text{wn}(B), \\ Y_t &= \mu_Y + CF_t + u_t, \quad u_t \sim \text{wn}(D). \end{aligned} \tag{22}$$

where $F_t \in \mathbb{R}^k$ is a mean-zero, stationary process with a stable transition matrix A, and $Y_t \in \mathbb{R}^n$ represents the observed cross-section. We assume the stochastic processes $\{e_t\}$ and $\{u_t\}$ are fundamental white noise innovations, satisfying the mutual orthogonality condition $E[u_t e_s'] = \mathbf{0}$ for all $s,t \in \mathbb{Z}$.

To identify the structural innovations ε_t, let $B = PP'$ denote the lower-triangular Cholesky decomposition of the state covariance matrix, with strictly positive diagonal elements $P_{ii} > 0$. The

structural shocks are defined via the linear transformation $e_t = P\varepsilon_t$, such that $E[\varepsilon_t \varepsilon_t'] = I_k$.

Finally, we define the regressor of interest x_t as the first element of both the state vector and the observation vector, $x_t = Y_t^1 = F_t^1$.

Theorem 1 (Latent SVAR Identification)**.** *Given the above set-up, consider the population regression coefficient from the local projection:*

$$Y_{j,t+h} = \alpha_{j,h} + \beta_{j,h}^{LP} x_t + \delta_{j,h}' F_{t-1} + \epsilon_{j,t+h}, \tag{23}$$

where $j \neq 1$ and $h \geq 0$. This is equivalent to the following:

$$\beta_{j,h}^{LP} = \frac{(CA^h P i_1)_j}{P_{11}}, \tag{24}$$

where i_1 is the first canonical basis vector.

Proof. Let $\tilde{z}$ denote the residual of a variable z projected on F_{t-1}. Under this notation, $\tilde{F}_t := F_t - AF_{t-1} = e_t$, which is white noise with covariance B. Moreover, the residual on the regressor of interest after conditioning on F_{t-1} is $\tilde{x}_t = i_1' e_t$. The h-step-ahead residual of the dependent variable is given by: $\tilde{Y}_{t+h} = CA^h e_t + \sum_{k=0}^{h-1} CA^k e_{t+h-k} + u_{t+h}$.

Observe that the population regression coefficient for observation Y_{t+h}^j is given by:

$$\beta_{j,h}^{LP}; = \frac{\mathrm{Cov}(\tilde{Y}_{t+h}^j, \tilde{x}_t)}{\mathrm{Cov}(\tilde{x}_t, \tilde{x}_t)} = \frac{\mathrm{Cov}(C_j A^h e_t, i_1' e_t)}{\mathrm{Cov}(i_1' e_t, i_1' e_t)} = \frac{C_j A^h B e_1}{e_1' B e_1}, \tag{25}$$

as it follows from the orthogonality conditions that only the term $CA^h e_t$ is correlated with $\tilde{x}_t$:

Now, from the Cholesky decomposition, $B = PP'$, note that $Be_1 = PP'e_1 = P(P_{11}e_1)$. Hence, $C_j A^h B e_1 = C_j A^h P e_1 P_{11}$ and $e_1' B e_1 = P_{11} P_{11}$. Canceling $P_{11} > 0$ gives $\beta_{j,h}^{LP} = \frac{(CA^h P e_1)_j}{P_{11}}$. □

The preceding theorem establishes that the estimand from a local projection can be recovered from the system matrices of the corresponding state-space model, provided the state innovations and measurement errors satisfy the mutual orthogonality condition. Critically, this equivalence holds in

population even when the latent factors are unobserved. Consequently, while the local projection as a one-step estimation is infeasible, we can still estimate the IRFs by estimating the transition and measurement equations. This joint estimation, however, is predicated on the global identifiability of the system; without sufficient structural constraints, the factor loading matrix C and the transition matrix A remain subject to rotational indeterminacy. To address this, the following theorem provides a sufficient condition for the unique identification of these matrices within the data.

Theorem 2. ***Global Identification of the System Matrices*** A ***and*** C**.** *Let the latent state-space system given by Equations 22 be minimal.*[16] *Suppose* Θ *is a parameter space such that for any non-singular matrix* $T \in \mathbb{R}^{k \times k}$*, the condition* $C(\theta)T^{-1} = C(\theta')$ *holds if and only if* $T = I_k$ *and* $\theta = \theta'$*, where* I_k *is the* $k \times k$ *identity matrix. Then, the system matrices* $A(\theta)$ *and* $C(\theta)$ *are globally identified.*

Proof. Let two sets of parameters, $\theta \in \Theta$ and $\theta' \in \Theta$, yield observationally equivalent state-space representations. In the context of linear Gaussian state-space models, observational equivalence implies that the two parameterizations generate an identical autocovariance generating function for the observation sequence $\{Y_t\}_{t \geq 1}$.

By standard system realization theory (Hannan and Deistler, 2012), two minimal linear systems are observationally equivalent if and only if their state vectors are related by a non-singular similarity transformation. Specifically, there must exist an invertible $k \times k$ matrix T such that the system matrices map to one another via:

$$A(\theta') = TA(\theta)T^{-1}. \tag{26}$$

$$C(\theta') = C(\theta)T^{-1}, \tag{27}$$

Substituting $T = I_k$ into the condition for the state transition matrix equivalence yields the requirement that $A(\theta') = A(\theta)$ and $C(\theta') = C(\theta)$. Because the transformation matrix is constrained

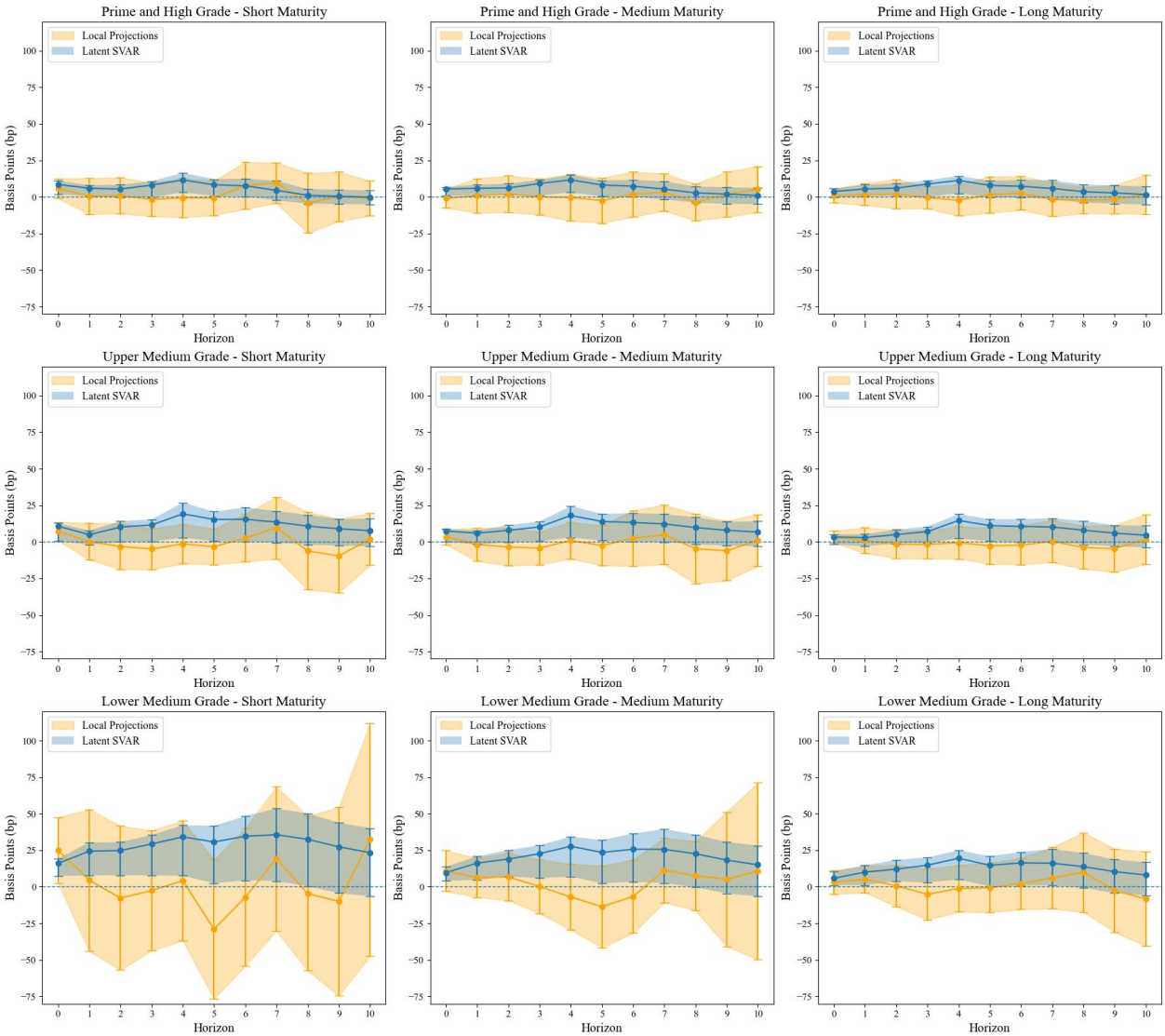
[16] Intuitively, a minimal system ensures that all states load onto Y and therefore influence the likelihood (observability) and that there are no "unreachable" states that do not respond to innovations (controllability). Minimality of linear state-space models is generic, so we do not prove that it holds for our Nelson-Siegel state-space model.

to be the identity matrix, no arbitrary rotations of the latent state-space can yield an observationally equivalent system. Consequently, θ is uniquely determined ($\theta = \theta'$), and the matrices $A(\theta)$ and $C(\theta)$ are uniquely and globally identified from the dynamic second moments of the data. $\square$

Following Theorem 2, the functional form of the Nelson-Siegel loadings—characterized by the unique monotonic decay of the slope component—ensures the global identification of the decay parameter λ and, consequently, the remaining system matrices. We then proceed to estimate the state-space system via maximum likelihood using the Kalman Filter; comprehensive details regarding the likelihood construction and optimization procedure are provided in Appendix B.1. Similar to the presentation in Figure 2, Figure 4 displays the resulting IRFs of credit spreads to a monetary policy shock across a three-by-three panel. In contrast to our previous study, here we define short, medium, and long maturities as the two-year, five-year, and ten-year spreads, respectively. To benchmark the performance of our Latent SVAR framework (in blue), each panel overlays the IRFs estimated via the local projection approach specified in Equation 16 (in orange).

Across all credit rating cohorts and maturity segments, the two estimation strategies yield broadly consistent point estimates, particularly at shorter horizons where the initial spread response is most pronounced. However, two clear differences emerge in terms of the standard errors associated with each estimation procedure and the persistence of the responses implied by the point estimates. Firstly, at longer horizons, the Latent SVAR achieves a significantly higher signal-to-noise ratio, evidenced by substantially narrower confidence intervals. As previously emphasized, this gain in efficiency stems from the state-space model's ability to pool information across the term structure and filter idiosyncratic measurement noise through the Nelson-Siegel cross-sectional restrictions. Secondly, the Latent SVAR identifies a more persistent policy transmission than the LP benchmark. While the horizon-by-horizon LP estimates are increasingly susceptible to estimation variance as the horizon increases, the Latent SVAR framework imposes a structural law of motion that captures an elevation in borrowing costs that is sustained across periods. This is underscored by the fact the credit spread response in the Latent SVAR framework is significantly positive across almost all maturities and credit ratings for several horizons, indicating a robust

Figure 4: Dynamic Causal Effects of Monetary Policy Shocks on the Term Structure of Credit Spreads



Note: This figure plots the impulse response functions of credit spreads to a one-standard-deviation monetary policy shock. The shock series is the "pure" monetary policy component identified by Jarociński and Karadi (2020). Columns correspond to maturity segments: short (2Y), medium (5Y), and long (10Y). Rows represent credit rating cohorts: Prime and High Grade, Upper Medium Grade, and Lower Medium Grade. The solid blue line denotes the Latent SVAR estimates based on Theorem 1; the solid orange line denotes the LP estimates from Equation 16 using the 2Y, 5Y, and 10Y yields and spreads as lagged controls. Shaded areas indicate 90% confidence intervals, constructed using a moving block bootstrap for the Latent SVAR and heteroskedasticity-consistent (HC3) standard errors for the local projections. The horizontal axis represents the forecast horizon in FOMC periods; the vertical axis measures the response in basis points.

and widespread tightening of credit conditions following a contractionary monetary shock.

Beyond gains in efficiency, the results once again demonstrate a clear structural monotonicity in policy transmission across both credit quality and maturity, although the differentials across

contemporaneous impulse responses is overall somewhat smaller for the Latent SVAR estimates compared to the LP estimates. As observed previously, spread sensitivity increases systematically as credit ratings deteriorate; Lower Medium Grade spreads exhibit a peak response of 25–40 basis points, approximately double the sensitivity observed in the Prime and High Grade cohorts. Within each rating category, we find a similar but less pronounced monotonic pattern across the term structure, with short-dated spreads displaying higher peak sensitivity than long-tenor counterparts. To ensure these results are robust to potential model misspecification - specifically the Gaussian assumption required for the Kalman filter - we employ a non-parametric moving block bootstrap using residuals derived from a Kalman smoother as described in Appendix B.2. This procedure generates the asymmetric, non-centered confidence intervals visible in the IRFs, accounting for the inherent heteroskedasticity and persistence of credit spread data. Rather than relying on asymptotic distributions that may not hold in finite samples with highly persistent states, this inferential framework ensures that our causal evidence remains robust while fully leveraging the structural advantages of the state-space representation.

5 Conclusion

Our empirical analysis demonstrates that monetary policy shocks exert a substantial influence on credit spreads of investment-grade corporate bonds. A one-standard-deviation monetary shock raises on average Treasury yields by 5 bps and credit spreads by 10 bps. We find that the magnitude of this transmission is heterogeneous across the credit spectrum and the term structure: the tightening effect is most pronounced for low-rated issuers (reaching 20 bps) and is relatively attenuated at longer maturities (close to 0). These findings are robust across a series of different monetary shock measurements and are structurally consistent with a theoretical framework of risky debt in which shocks to the short-term risk-free rate are negatively correlated with the firm's underlying value process. Under this intuition, shock propagation is amplified for distressed debt characterized by higher idiosyncratic volatility, yet mitigated for long-duration instruments where

the present value of the terminal claim is less sensitive to transitory policy innovations. While the structural origins of this negative correlation remain an open question for future research, our results provide a robust empirical benchmark for such theoretical extensions.

From a methodological perspective, we show that although corporate bond yields are inherently noisy due to illiquidity and thin trading volumes, inferential efficiency may be gained by exploiting the latent factor structure of the joint term structures in an approach that we call Latent SVAR. As is true for Treasury yields, we demonstrate that credit spreads admit a low-dimensional factor representation where the factors can be interpreted as a level, slope, and curvature. This general state-space procedure facilitates a rigorous dimension-reduction that preserves the signal-to-noise ratio in the cross-section of spreads — a framework that we believe holds broad applicability for other domains in empirical asset pricing and macro-finance.

For policymakers, these results highlight the marked heterogeneity in the transmission of monetary policy to firm-level funding costs. While this study does not directly map these cost-of-capital fluctuations to real investment decisions, it provides a necessary first step in quantifying how a firm's creditworthiness and funding horizon dictate its exposure to policy shocks. A monetary stance that is cognizant of its differential impact on private sector financing can play a vital role in preventing inefficient defaults and preserving productive capacity.

Furthermore, our findings offer unique insights for fixed-income practitioners by quantifying the term-structure risks inherent in credit portfolios. Beyond standard duration and credit-spread sensitivities, we identify a distinct source of uncertainty stemming from the monetary policy announcements which appear to impact the medium-to-long end of the yield curve and the short-to-medium end of the spread curves the most. By mapping these dynamics, our framework offers a systematic basis for constructing more precise hedges against monetary policy shocks, ultimately improving risk management for diversified credit mandates.

References

Acosta, M., Ajello, A., Bauer, M. D., Loria, F., and Miranda-Agrippino, S. (2025). Financial market effects of fomc communication: Evidence from a new event-study database. Technical report, IMFS Working Paper Series.

Adrian, T., Crump, R. K., and Vogt, E. (2019). Nonlinearity and flight-to-safety in the risk-return trade-off for stocks and bonds. *The Journal of Finance*, 74(4):1931–1973.

Ang, A. and Piazzesi, M. (2003). A no-arbitrage vector autoregression of term structure dynamics with macroeconomic and latent variables. *Journal of Monetary economics*, 50(4):745–787.

Bauer, M. D. and Swanson, E. T. (2023a). An alternative explanation for the "fed information effect". *American Economic Review*, 113(3):664–700.

Bauer, M. D. and Swanson, E. T. (2023b). A reassessment of monetary policy surprises and high-frequency identification. *NBER Macroeconomics Annual*, 37(1):87–155.

Becker, B. and Ivashina, V. (2015). Reaching for yield in the bond market. *The Journal of Finance*, 70(5):1863–1902.

Bernanke, B. S., Gertler, M., and Gilchrist, S. (1999). The financial accelerator in a quantitative business cycle framework. *Handbook of macroeconomics*, 1:1341–1393.

Bernanke, B. S. and Kuttner, K. N. (2005). What explains the stock market's reaction to federal reserve policy? *The Journal of finance*, 60(3):1221–1257.

Bessembinder, H. and Maxwell, W. (2008). Markets: Transparency and the corporate bond market. *Journal of economic perspectives*, 22(2):217–234.

Black, F. and Scholes, M. (1973). The pricing of options and corporate liabilities. *Journal of political economy*, 81(3):637–654.

Bolton, P., Freixas, X., and Shapiro, J. (2012). The credit ratings game. *The Journal of Finance*, 67(1):85–111.

Christensen, J. H., Diebold, F. X., and Rudebusch, G. D. (2011). The affine arbitrage-free class of nelson–siegel term structure models. *Journal of Econometrics*, 164(1):4–20.

Collin-Dufresne, P., Goldstein, R. S., and Martin, J. S. (2001). The determinants of credit spread changes. *The Journal of Finance*, 56(6):2177–2207.

Cook, T. and Hahn, T. (1989). The effect of changes in the federal funds rate target on market interest rates in the 1970s. *Journal of monetary economics*, 24(3):331–351.

Dick-Nielsen, J. (2014). How to clean enhanced trace data. *Available at SSRN 2337908*.

Diebold, F. X. and Li, C. (2006). Forecasting the term structure of government bond yields. *Journal of econometrics*, 130(2):337–364.

Diebold, F. X., Rudebusch, G. D., and Aruoba, S. B. (2006). The macroeconomy and the yield curve: a dynamic latent factor approach. *Journal of econometrics*, 131(1-2):309–338.

Drechsler, I., Savov, A., and Schnabl, P. (2018). A model of monetary policy and risk premia. *The Journal of Finance*, 73(1):317–373.

Driscoll, J. C. and Kraay, A. C. (1998). Consistent covariance matrix estimation with spatially dependent panel data. *Review of economics and statistics*, 80(4):549–560.

Duffee, G. R. (1998). The relation between treasury yields and corporate bond yield spreads. *The Journal of Finance*, 53(6):2225–2241.

Duffie, D. and Kan, R. (1996). A yield-factor model of interest rates. *Mathematical finance*, 6(4):379–406.

Friewald, N., Jankowitsch, R., and Subrahmanyam, M. G. (2012). Illiquidity or credit deterioration: A study of liquidity in the us corporate bond market during financial crises. *Journal of financial economics*, 105(1):18–36.

Geman, H., El Karoui, N., and Rochet, J.-C. (1995). Changes of numeraire, changes of probability measure and option pricing. *Journal of Applied probability*, 32(2):443–458.

Gertler, M. and Karadi, P. (2015). Monetary policy surprises, credit costs, and economic activity. *American Economic Journal: Macroeconomics*, 7(1):44–76.

Gilchrist, S. and Zakrajšek, E. (2012). Credit spreads and business cycle fluctuations. *American economic review*, 102(4):1692–1720.

Gürkaynak, R. S., Sack, B., and Swansonc, E. T. (2005). Do actions speak louder than words? the response of asset prices to monetary policy actions and statements. *International Journal of Central Banking*.

Hannan, E. and Deistler, M. (2012). *The Statistical Theory of Linear Systems*, volume 70. SIAM.

Hanson, S. G. and Stein, J. C. (2015). Monetary policy and long-term real rates. *Journal of Financial Economics*, 115(3):429–448.

Heath, D., Jarrow, R., and Morton, A. (1992). Bond pricing and the term structure of interest rates: A new methodology for contingent claims valuation. *Econometrica: Journal of the Econometric Society*, pages 77–105.

Hull, J. and White, A. (1990). Pricing interest-rate-derivative securities. *The review of financial studies*, 3(4):573–592.

Jarociński, M. and Karadi, P. (2020). Deconstructing monetary policy surprises—the role of information shocks. *American Economic Journal: Macroeconomics*, 12(2):1–43.

Jarrow, R. A., Lando, D., and Turnbull, S. M. (1997). A markov model for the term structure of credit risk spreads. *The review of financial studies*, 10(2):481–523.

Jordà, Ò. (2005). Estimation and inference of impulse responses by local projections. *American economic review*, 95(1):161–182.

Joslin, S., Le, A., and Singleton, K. J. (2013). Why gaussian macro-finance term structure models are (nearly) unconstrained factor-vars. *Journal of Financial Economics*, 109(3):604–622.

Joslin, S., Singleton, K. J., and Zhu, H. (2011). A new perspective on gaussian dynamic term structure models. *The Review of Financial Studies*, 24(3):926–970.

Kuttner, K. N. (2001). Monetary policy surprises and interest rates: Evidence from the fed funds futures market. *Journal of monetary economics*, 47(3):523–544.

Leland, H. E. and Toft, K. B. (1996). Optimal capital structure, endogenous bankruptcy, and the term structure of credit spreads. *The journal of finance*, 51(3):987–1019.

Litterman, R. (1991). Common factors affecting bond returns. *Journal of fixed income*, pages 54–61.

Longstaff, F. A. and Schwartz, E. S. (1995). A simple approach to valuing risky fixed and floating rate debt. *The Journal of Finance*, 50(3):789–819.

Merton, R. C. (1973). Theory of rational option pricing. *The Bell Journal of Economics and Management Science*, 4(1):141–183.

Merton, R. C. (1974). On the pricing of corporate debt: The risk structure of interest rates. *The Journal of finance*, 29(2):449–470.

Miranda-Agrippino, S. and Ricco, G. (2021). The transmission of monetary policy shocks. *American Economic Journal: Macroeconomics*, 13(3):74–107.

Montiel Olea, J. L. and Plagborg-Møller, M. (2021). Local projection inference is simpler and more robust than you think. *Econometrica*, 89(4):1789–1823.

Nakamura, E. and Steinsson, J. (2018). High-frequency identification of monetary non-neutrality: the information effect. *The Quarterly Journal of Economics*, 133(3):1283–1330.

Nelson, C. R. and Siegel, A. F. (1987). Parsimonious modeling of yield curves. *Journal of business*, pages 473–489.

Nualart, D. (2006). *The Malliavin calculus and related topics*. Springer.

Ottonello, P. and Winberry, T. (2020). Financial heterogeneity and the investment channel of monetary policy. *Econometrica*, 88(6):2473–2502.

Plagborg-Møller, M. and Wolf, C. K. (2021). Local projections and vars estimate the same impulse responses. *Econometrica*, 89(2):955–980.

Rigobon, R. and Sack, B. (2004). The impact of monetary policy on asset prices. *Journal of monetary economics*, 51(8):1553–1575.

Sarig, O. and Warga, A. (1989). Some empirical estimates of the risk structure of interest rates. *The Journal of Finance*, 44(5):1351–1360.

Shimko, D. C., Tejima, N., and Van Deventer, D. R. (1993). The pricing of risky debt when interest rates are stochastic. *The Journal of Fixed Income*, 3(2):58–65.

Stock, J. H. and Watson, M. W. (2016). Dynamic factor models, factor-augmented vector autoregressions, and structural vector autoregressions in macroeconomics. In *Handbook of macroeconomics*, volume 2, pages 415–525. Elsevier.

Sundaresan, S. (2013). A review of merton's model of the firm's capital structure with its wide applications. *Annu. Rev. Financ. Econ.*, 5(1):21–41.

Vasicek, O. (1977). An equilibrium characterization of the term structure. *Journal of financial economics*, 5(2):177–188.

Vayanos, D. and Vila, J.-L. (2021). A preferred-habitat model of the term structure of interest rates. *Econometrica*, 89(1):77–112.

A Derivations in the Merton-Style Model of Debt

A.1 Derivation of the Corporate Bond Price

As demonstrated by Equation 4, to solve for the price of the corporate bond $D_K(t,T)$, we only need to derive the call price $C_K(t,T)$. This is the price of a European call option on the value of the firm, given the same maturity T and where the strike price is set to be the face value of the debt K.

Under the risk-neutral measure $\mathbb{Q}$, this price is given by:

$$C_K(t,T) = \mathbb{E}^{\mathbb{Q}}\left[e^{-\int_t^T r_s ds}(V_T - K)^+ \middle| \mathcal{F}_t\right], \tag{28}$$

where the dynamics of V_t and r_t are expressed by Equations 1, 2, and 3. However, solving this expectation directly is difficult because the payoff depends on the joint distribution of the firm value V_t and the stochastic discount factor generated by the short rate process r_t. Instead, we apply the change-of-numeraire technique introduced by Geman et al. (1995).

First, let us define the T-forward measure $\mathbb{Q}^T$ via the Radon–Nikodym derivative:

$$\frac{d\mathbb{Q}^T}{d\mathbb{Q}}\Big|_{\mathcal{F}_t} = \frac{\frac{P(t,T)}{M_t}}{\frac{P(0,T)}{M_0}}, \tag{29}$$

where $M_t = e^{\int_0^t r_s ds}$ denotes the money-market account, which serves as the numeraire under $\mathbb{Q}$.

Under this measure, the expression for the call price in 28 can be rewritten as:

$$C_K(t,T) = P(t,T)\mathbb{E}^{\mathbb{Q}^T}\left[(V_T - K)^+ \middle| \mathcal{F}_t\right]. \tag{30}$$

Next, let us define the T-forward price of the firm value:

$$F_t := \frac{V_t}{P(t,T)}. \tag{31}$$

By Itô's lemma and Girsanov's theorem, this process is a martingale under the T-forward measure

$\mathbb{Q}^T$:

$$\frac{dF_t}{F_t} = \sigma_F(t,T)dW_t^T, \tag{32}$$

where W_t^T is a Brownian motion under $\mathbb{Q}^T$, and the time-dependent volatility of the forward price is

$$\sigma_F^2(t,T) = \sigma_V^2 + \sigma_P^2(t,T) + 2\rho\sigma_V\sigma_P(t,T), \tag{33}$$

where $\sigma_P(t,T)$ is the A(t,T)-coupon bond price given by the Vasicek model:

$$\sigma_P(t,T) = \sigma_r B(t,T) = \frac{\sigma_r}{\kappa}\left(1 - e^{-\kappa(T-t)}\right). \tag{34}$$

Under $\mathbb{Q}^T$, the forward price at time T conditional on the time-t filtration is distributed as follows:

$$\ln F_T | \mathcal{F}_t \sim \mathcal{N}\left(\ln F_t - \frac{1}{2}\int_t^T \sigma_F^2(s,T)ds, \int_t^T \sigma_F^2(s,T)ds\right). \tag{35}$$

Therefore, the call price can be obtained by applying the Black–Scholes–Merton formula with integrated variance:

$$C_K(t,T) = P(t,T)\Big[F_t N(d_1) - K N(d_2)\Big], \tag{36}$$

where

$$d_1 = \frac{\ln(F_t/K) + \frac{1}{2}\int_t^T \sigma_F^2(s,T)ds}{\sqrt{\int_t^T \sigma_F^2(s,T)ds}}, \tag{37}$$

$$d_2 = d_1 - \sqrt{\int_t^T \sigma_F^2(s,T)ds}, \tag{38}$$

and F_t and $\sigma_F(t,T)$ are given by Equations 31 and 33 respectively.

A.2 Derivation of the Malliavin Derivative of the Credit Spread With Respect to Monetary Policy Shocks

From Equation 8, it follows that the corresponding credit spread is given by:

$$s(t,T) = -\frac{1}{\tau}\ln\left(\frac{V_t(1-N(d_1))}{KP(t,T)} + N(d_2)\right). \tag{39}$$

To solve for the Malliavin derivative $\mathcal{D}_t^r s(t,T)$, let us define the following:

$$X(t,T) := \frac{V_t}{KP(t,T)} = \frac{V_t}{K}\exp\big(B(t,T)r_t - A(t,T)\big). \tag{40}$$

This is the forward moneyness of the underlying asset price V_t for maturity T. From the chain rule, it follows that:

$$\mathcal{D}_t^r X(t,T) = X(t,T)\big(\rho\sigma_V + B(t,T)\sigma_r\big). \tag{41}$$

Lemma 1. *Let $\varphi(\cdot)$ denote the probability density function of the standard normal distribution. $X(t,T)\varphi(d_1) = \varphi(d_2)$.*

Proof. Observe that $\frac{\varphi(d_2)}{\varphi(d_1)} = e^{\frac{(d_1+d_2)(d_1-d_2)}{2}}$, where:

$$d_1 + d_2 = \frac{2\ln(\frac{F_t}{K})}{\sqrt{\int_t^T \sigma_F^2(s,T)ds}}, \tag{42}$$

and

$$d_1 - d_2 = \sqrt{\int_t^T \sigma_F^2(s,T)ds}. \tag{43}$$

It follows that $\frac{\varphi(d_2)}{\varphi(d_1)} = X(t,T)$. □

After substituting the above into our expression for the credit spread, we again apply the chain rule and find that:

$$
\begin{aligned}
\mathcal{D}_t^r s_t(\tau) &= \mathcal{D}_t^r \left(-\frac{1}{\tau} \ln\Big(X(t,T)\big(1-N(d_1)\big) + N(d_2) \Big) \right), \\
&= -\frac{1}{\tau} \frac{KP_t}{D_t} \mathcal{D}_t^r \Big(X_t\big(1-N(d_1)\big) + N(d_2) \Big), \\
&= -\frac{1}{\tau} \frac{KP_t}{D_t} \left[X_t\big(\rho\sigma_V + B_t\sigma_r\big)\big(1-N(d_1)\big) - X_t \frac{\varphi(d_1)\big(\rho\sigma_V + B_t\sigma_r\big)}{\sqrt{\int_t^T \sigma_F^2(s,T)ds}} + \frac{\varphi(d_2)\big(\rho\sigma_V + B_t\sigma_r\big)}{\sqrt{\int_t^T \sigma_F^2(s,T)ds}} \right], \\
&= -\frac{1}{\tau} \frac{V_t}{D_t} \big(\rho\sigma_V + B_t\sigma_r\big)\big(1-N(d_1)\big),
\end{aligned}
\tag{44}
$$

where the final equality follows from Lemma 1 and we suppress notation for $B(t,T)$, $P(t,T)$, and $X(t,T)$ for convenience.

A.3 Derivation of the Partial Derivatives of the Malliavin Derivative

A.3.1 Partial Derivative with Respect to the Volatility of the Value Process

First, we derive the partial derivative of the Malliavin derivative $\mathcal{D}_t^r s_t(\tau)$ with respect to the volatility of the value process σ_V. By the product rule and chain rule, we have that:

$$
\frac{\partial \mathcal{D}_t^r s_t(\tau)}{\partial \sigma_V} = -\frac{V_t}{\tau} \left[\rho \frac{1-N(d_1)}{D_t} - (\rho\sigma_V + B_t\sigma_r) \frac{\varphi(d_1) D_t \frac{\partial d_1}{\partial \sigma_V} + (1-N(d_1)) \frac{\partial D_t}{\partial \sigma_V}}{D_t^2} \right], \tag{45}
$$

where

$$
\frac{\partial d_1}{\partial \sigma_V} = \frac{\frac{1}{4}\int_t^T (2\sigma_V + 2\rho\sigma_r B_s) ds \sqrt{\int_t^T \sigma_F^2(s,T)ds} - \frac{\ln(\frac{F_t}{K}) \int_t^T (2\sigma_V + 2\rho\sigma_r B_s) ds}{2\sqrt{\int_t^T \sigma_F^2(s,T)ds}}}{\int_t^T \sigma_F^2(s,T)ds}, \tag{46}
$$

and

$$\begin{aligned}\frac{\partial D_t}{\partial \sigma_V} &= -V_t\varphi(d_1)\frac{\partial d_1}{\partial \sigma_V} + KP(t,T)\varphi(d_2)\frac{\partial d_2}{\partial \sigma_V},\\ &= V_t\varphi(d_1)\left(\frac{\partial d_2}{\partial \sigma_V} - \frac{\partial d_1}{\partial \sigma_V}\right),\\ &= -\frac{V_t\varphi(d_1)\int_t^T(2\sigma_V + 2\rho\sigma_r B_s)ds}{2\sqrt{\int_t^T \sigma_F^2 ds}},\end{aligned} \tag{47}$$

for which the second equality follows from Lemma 1 and the third follows from taking the partial derivatives of both sides of Equation 38.

For ρ such that $\rho\sigma_V + B_t\sigma_r < 0$, the sign of the $\frac{\partial \mathcal{D}_t^r s_t(\tau)}{\partial \sigma_V}$ crucially depends on the sign of $\frac{\partial d_1}{\partial \sigma_V}$ as $\frac{\partial D_t}{\partial \sigma_V}$ is non-positive. In particular, observe that if $\frac{1}{2}\int_t^T \sigma_F^2 ds < \ln(\frac{F_t}{K})$, then $\frac{\partial d_1}{\partial \sigma_V}$ is negative and $\frac{\partial \mathcal{D}_t^r s_t(\tau)}{\partial \sigma_V}$ is positive.

A.3.2 Partial Derivative with Respect to the Maturity of the Corporate Bond

To compute the partial derivative with respect to maturity τ, we apply the product and chain rules again:

$$\begin{aligned}\frac{\partial \mathcal{D}_t^r s_t(\tau)}{\partial \tau} = &\frac{1}{\tau^2}\frac{V_t}{D_t}(\rho\sigma_V + B_t\sigma_r)\big(1 - N(d_1)\big) - \frac{1}{\tau}\frac{\sigma_r V_t(1 - N(d_1))}{D_t}\frac{\partial B_t}{\partial \tau}\\ &+ \frac{V_t}{\tau}(\rho\sigma_V + B_t\sigma_r)\frac{\varphi(d_1)D_t\frac{\partial d_1}{\partial \tau} + (1 - N(d_1))\frac{\partial D_t}{\partial \tau}}{D_t^2},\end{aligned} \tag{48}$$

where

$$\frac{\partial B_t}{\partial \tau} = B'(\tau) = e^{-\kappa\tau}, \tag{49}$$

$$\frac{\partial D_t}{\partial \tau} = -\frac{V_t\varphi(d_1)}{2\sqrt{\int_t^T \sigma_F^2(s,T)ds}}\left(\sigma_V^2 + \int_t^T \frac{\partial \sigma_F^2}{\partial \tau}ds\right) + K\frac{\partial P_t}{\partial \tau}N(d_2), \tag{50}$$

$$\frac{\partial d_1}{\partial \tau} = \frac{\left(\frac{1}{4}\big(\sigma_V^2 + \int_t^T \frac{\partial \sigma_F^2}{\partial \tau}ds\big) - \frac{1}{P_t}\frac{\partial P_t}{\partial \tau}\right)\sqrt{\int_t^T \sigma_F^2(s,T)ds} - \frac{\ln\left(\frac{F_t}{K}\right)\left(\sigma_V^2 + \int_t^T \frac{\partial \sigma_F^2}{\partial \tau}ds\right)}{2\sqrt{\int_t^T \sigma_F^2(s,T)ds}}}{\int_t^T \sigma_F^2(s,T)ds}, \tag{51}$$

$$\frac{\partial P_t}{\partial \tau} = P_t\Big((\theta - \frac{\sigma_r^2}{2\kappa^2})(B'(\tau) - 1) - \frac{\sigma_r^2}{2\kappa}B(\tau)B'(\tau) - B'(\tau)r_t\Big), \tag{52}$$

and

$$\frac{\partial \sigma_F^2}{\partial \tau} = 2\sigma_r^2 B(\tau) B'(\tau) + 2\rho\sigma_V \sigma_r B'(\tau). \tag{53}$$

Observe that the first two terms in the sum in Equation 48 are negative when $\rho\sigma_V + b_t\sigma_r < 0$ but the sign of the last term is positive when the forward moneyness is large. Consequently, the sign of $\frac{\partial \mathcal{D}_t^r s_t(\tau)}{\partial \tau}$ is largely indeterminate.

A.4 Asymptotic Behavior of the Malliavin Derivative

A.4.1 Asymptotic Behavior with Respect to the Volatility of the Value Process

From the forward volatility specification in Equation 33,

$$\int_t^T \sigma_F^2(s,T)ds = \sigma_V^2 \tau + O(\sigma_V) + O(1). \tag{54}$$

Consequently, using the definition in Equation 37,

$$d_1 = \frac{\ln(F_t/K) + \frac{1}{2}\int_t^T \sigma_F^2(s,T)ds}{\sqrt{\int_t^T \sigma_F^2(s,T)ds}} = \frac{1}{2}\sigma_V\sqrt{\tau} + O(1), \tag{55}$$

and therefore

$$d_2 = d_1 - \sqrt{\int_t^T \sigma_F^2(s,T)ds} = -\frac{1}{2}\sigma_V\sqrt{\tau} + O(1). \tag{56}$$

Hence $d_1 \to \infty$ and $d_2 \to -\infty$ as $\sigma_V \to \infty$. Applying Mills' ratio yields

$$1 - N(d_1) = O\left(\frac{\varphi(d_1)}{d_1}\right), \qquad N(d_2) = O\left(\frac{\varphi(d_2)}{|d_2|}\right). \tag{57}$$

Since $\varphi(d_1) = \varphi(d_2)$ and $d_1, |d_2| = O(\sigma_V)$, it follows that

$$1 - N(d_1) = O\left(\frac{e^{-c\sigma_V^2}}{\sigma_V}\right), \qquad N(d_2) = O\left(\frac{e^{-c\sigma_V^2}}{\sigma_V}\right) \tag{58}$$

for some constant $c>0$. Thus

$$D_t = V_t(1-N(d_1)) + KP(t,T)N(d_2) = O\left(\frac{e^{-c\sigma_V^2}}{\sigma_V}\right). \tag{59}$$

Moreover,

$$\frac{1-N(d_1)}{D_t} = O(1), \tag{60}$$

since both terms in D_t vanish at the same exponential rate.

Substituting into the expression for the Malliavin derivative in Equation 14 gives

$$\mathcal{D}_t^r s_t(\tau) = -\frac{V_t}{\tau}(\rho\sigma_V + B(t,T)\sigma_r)O(1). \tag{61}$$

When ρ is assumed to be negative,

$$\mathcal{D}_t^r s_t(\tau) = O(\sigma_V) \qquad \text{as } \sigma_V \to \infty. \tag{62}$$

Thus, the magnitude of the Malliavin derivative grows linearly with σ_V and tends to positive infinity.

A.4.2 Asymptotic Behavior with Respect to the Maturity of the Corporate Bond

For the Vasicek zero-coupon bond price in Equation 5, we have

$$B(t,T) = \frac{1-e^{-\kappa\tau}}{\kappa} = \frac{1}{\kappa} + O(e^{-\kappa\tau}), \quad P(t,T) = O(e^{-c\tau}), \quad c>0. \tag{63}$$

Hence, the forward price satisfies

$$F_t = \frac{V_t}{P(t,T)} = O(e^{c\tau}), \tag{64}$$

which implies

$$\ln(F_t/K) = O(\tau). \tag{65}$$

On the other hand, the integrated variance satisfies

$$\int_t^T \sigma_F^2(s,T)ds = O(\tau), \tag{66}$$

so that the numerator of d_1 is $O(\tau)$ and the denominator is $O(\sqrt{\tau})$. Consequently,

$$d_1 = O(\sqrt{\tau}), \qquad d_2 = O(\sqrt{\tau}). \tag{67}$$

Applying Mills' ratio for the Gaussian tail yields

$$1 - N(d_1) \leq \frac{\varphi(d_1)}{d_1}, \quad \varphi(x) = \frac{1}{\sqrt{2\pi}} e^{-x^2/2}. \tag{68}$$

Since $d_1^2 = \Theta(\tau)$ for large τ, it follows that

$$1 - N(d_1) = O(e^{-C\tau}), \quad C > 0. \tag{69}$$

The denominator satisfies

$$D_t = V_t(1 - N(d_1)) + KP(t,T)N(d_2) = O(e^{-C\tau}) + O(e^{-c\tau}) = O(e^{-\min(C,c)\tau}), \tag{70}$$

while the numerator behaves as

$$V_t(\rho\sigma_V + B(t,T)\sigma_r)(1 - N(d_1)) = O(e^{-C\tau}). \tag{71}$$

Hence, the ratio of numerator to denominator is bounded as follows:

$$\frac{V_t(\rho\sigma_V + B(t,T)\sigma_r)(1 - N(d_1))}{D_t} = O(1), \tag{72}$$

where we have used that the exponentially small τ-dependence in $B(t,T)$ does not affect the leading-order Big-O.

Including the $1/\tau$ prefactor in $\mathcal{D}_t^r s_t(\tau)$ gives

$$\mathcal{D}_t^r s_t(\tau) = -\frac{1}{\tau}\frac{V_t(\rho\sigma_V + B(t,T)\sigma_r)(1-N(d_1))}{D_t} = O\Big(\frac{1}{\tau}\Big) \to 0, \quad \tau \to \infty. \tag{73}$$

Therefore, we conclude that

$$\lim_{\tau\to\infty} \mathcal{D}_t^r s_t(\tau) = 0. \tag{74}$$

B Latent SVAR Estimation and Inference

B.1 Kalman Filter-Based Maximum Likelihood Estimation

In this section, we provide an algorithm for estimating the state matrices described in the latent state-space model in Equation 22. To begin, let us use the superscript notation to define the history of a variable: for example, $Y^{t-1} = \{Y_{t-1},...,Y_0\}$. We use the subscript $t|t-1$ meanwhile to denote the conditional mean of the variable at time t with respect to the observed history up until time $t-1$: for example, $F_{t|t-1} = E[F_t|Y^{t-1}]$. Let $U_{t|t-1} = E\Big[\big(F_t - F_{t|t-1}\big)\big(F_t - F_{t|t-1}\big)'|Y^{t-1}\Big]$ be the conditional variance of the latent factor at time t. From this, we can solve for and define the following:

$$Y_{t|t-1} = E\big[Y_t\big|Y^{t-1}\big] = E\big[\mu_Y + CF_t + u_t\big|y^{t-1}\big] = \mu_Y + CF_{t|t-1} \tag{75}$$

$$V_{t|t-1} = E\Big[\big(Y_t - Y_{t|t-1}\big)\big(Y_t - Y_{t|t-1}\big)'\Big|Y^{t-1}\Big] = CU_{t|t-1}C' + D \tag{76}$$

$$E\Big[\big(Y_t - Y_{t|t-1}\big)\big(F_t - F_{t|t-1}\big)'\Big|Y^{t-1}\Big] = CU_{t|t-1} \tag{77}$$

Now, for any given set of parameters θ, we denote the log-likelihood function evaluated at θ as follows: $l\big(\theta|Y^T\big) = p\big(Y^T|\theta\big)$, where p is the log of the probability density function of Y^T. This is a log joint density function that we can separate out into conditional densities: $p\big(Y^T|\theta\big) = p\big(Y_T\big|Y^{T-1},\theta\big) + ... + p(Y_1|Y^0,\theta) + p(Y_0|\theta)$. We fix some initial value for $F_{0|0}$ and $P_{0|0}$ and

let the marginal distribution of F_0 be given by $F_0 \sim N\left(F_{0|0}, P_{0|0}\right)$. Moreover, we initialize $l(\theta|Y^0)$ equal to 0. From θ, we can construct μ_Y, A, B, C, and D. For t between time dates 1 to T, we perform the following. We begin by forecasting the states and errors on the states:

$$F_{t|t-1} = AF_{t-1|t-1} \tag{78}$$

$$U_{t|t-1} = BP_{t-1|t-1}B' + \Pi \tag{79}$$

We subsequently forecast the observables and the errors on the observables. This is given by Equations 75 and 76 respectively. Since $Y_t|Y^{t-1} \sim N\left(Y_{t|t-1}, V_{t|t-1}\right)$, the log likelihood function can hence be updated as follows:

$$l\left(\theta\middle|Y^{t+1}\right) = l\left(\theta\middle|Y^t\right) - \frac{1}{2}\left(ln\left(\left|V_{t|t-1}\right|\right) + \left(Y_t - Y_{t|t-1}\right)' V_{t|t-1}^{-1}\left(Y_t - Y_{t|t-1}\right)\right). \tag{80}$$

Now, observe that the joint distribution of the latent factors and the observations at t given the observed history up to time $t-1$ is given by:

$$\begin{bmatrix} F_t \\ Y_t \end{bmatrix} \middle| Y^{t-1} \sim N\left(\begin{bmatrix} F_{t|t-1} \\ Y_{t|t-1} \end{bmatrix}, \begin{bmatrix} U_{t|t-1} & U_{t|t-1}C' \\ CU_{t|t-1} & V_{t|t-1} \end{bmatrix}\right). \tag{81}$$

From this, the conditional distribution of the latent factor at time t given the observed history up to time t is:

$$F_t|Y^t = F_t|Y_t, Y^{t-1} \sim N\left(F_{t|t-1} + U_{t|t-1}C'V_{t|t-1}^{-1}\left(Y_t - Y_{t|t-1}\right)', U_{t|t-1} - U_{t|t-1}C'V_{t|t-1}^{-1}CU_{t|t-1}\right). \tag{82}$$

Let us denote the Kalman gain by $K_{t|t-1} = U_{t|t-1}C'V_{t|t-1}^{-1}$ the Kalman gain. The updated forecasts of the states are given by:

$$F_{t|t} = F_{t|t-1} + K_{t|t-1}\left(Y_t - Y_{t|t-1}\right), \tag{83}$$

$$U_{t|t} = U_{t|t-1} - K_{t|t-1}CU_{t|t-1}. \tag{84}$$

We implement this algorithm in JAX, a high-performance numerical computing library in Python, and use a solver to minimize the negative log-likelihood function. We define convergence in the parameters as when the relative improvement in log-likelihood $\frac{l_{k+1}-l_k}{1+|l_k|}$ drops below 10^8. For a given iteration of the parameters θ, we set $F_{0|0}$ to the unconditional mean μ_F and adopt a quasi-diffuse initialization for $U_{0|0}$. We additionally include a burn-in of 10 periods to reduce initialization bias, after which we then start computing the log-likelihood function. This is a longer burn-in than what is commonly used in maximum likelihood estimation of state-space models; however, our observations, namely Treasury and corporate yields, are highly persistent. Consequently, a longer burn-in period is necessary to account for the initialization bias.

Additionally, our implementation differs slightly from the general approach laid out above to account for both numerical stability and missing observations. For numerical stability, we update on the Cholesky roots of the covariance matrices rather than the matrices directly. Moreover, we add a small amount of jitter when we recover the covariance matrices. Both measures help ensure positive semi-definiteness for when we later take inverses of the covariance matrices. To account for missingness, one possibility is to omit these observations and resize the system matrices C and D accordingly. This, however, slows down the implementation in JAX and means that we cannot leverage the full benefits of just-in-time compilation. Consequently, we adopt instead the following simple numerical approximation, which preserves the size and initialization of the system matrices. Let M_t be an indicator vector where the i^{th} element of M_t is one if the i^{th} element of Y_t is missing and zero otherwise. We adjust the prediction step of the covariance matrix on the observations in 76 as follows:

$$V_{t|t-1} = CU_{t|t-1}C' + D + \psi \cdot \text{diag}(M_t), \tag{85}$$

where ψ is initialized at some large value. Here, missing entries are accounted for by a large variance term, which results in them effectively being ignored in the likelihood updating.

B.2 Kalman Smoother-Based Estimation of the Latent Residuals

After obtaining the maximum likelihood estimates for the parameters θ, we can then recover the time series of the latent state variables and their residuals using a Kalman smoother. This is a two-pass algorithm: in the forward pass, we estimate the states using the contemporaneous history of observations at time t with the Kalman filter as described in the prior section; in the backward pass, we refine the state estimates using the full history up to time T. Given the state mean and covariance estimates $\{F_{t|t}\}_{t=0}^{T}$ and $\{U_{t|t}\}_{t=0}^{T}$ derived from the Kalman filter, we proceed in this section by describing the estimation of $\{F_{t|T}\}_{t=0}^{T}$ using the Kalman smoother.

Thus, starting at the last time period T and working backwards to time $t=0$, we begin by noting that the conditional autocovariance of the latent factors are given by:

$$E\Big[\big(F_{t+1}-F_{t+1|t}\big)\big(F_t-F_{t|t}\big)'\Big|Y^t\Big]=BU_{t|t} \tag{86}$$

From this, we can express the joint distribution of the factors as follows:

$$\begin{bmatrix}F_t\\F_{t+1}\end{bmatrix}\Big|Y^t\sim N\left(\begin{bmatrix}F_{t|t}\\F_{t+1|t}\end{bmatrix},\begin{bmatrix}U_{t|t} & U_{t|t}B'\\BU_{t|t} & P_{t+1|t}\end{bmatrix}\right). \tag{87}$$

Again, we can extract out the conditional distribution from this multivariate normal distribution as follows:

$$F_t|F_{t+1},Y^t\sim N\Big(F_{t|t}+U_{t|t}B'P_{t+1|t}^{-1}(F_{t+1|T}-f_{t+1|t}),U_{t|t}-V_{t|t}B'P_{t+1|t}^{-1}BU_{t|t}\Big) \tag{88}$$

Let us denote the gain from the smoother as $G_t=U_{t|t}B'P_{t+1|t}^{-1}$. Observe that since the full history of observations can be expressed as $Y^T=g(Y^t,F_t,u_{t+1},e_{t+1},...,u_T,e_T)$ for some function $g(\cdot)$ and

all future innovations are independent of F_t, it follows from the law of iterated expectations that:

$$F_{t|T} = E\big[E\big[F_t\big|F_{t+1}, Y^t\big]\big|Y^T\big] \tag{89}$$

$$= E\big[F_{t|t} + G_t(F_{t+1|T} - F_{t+1|t})\big|Y^T\big] \tag{90}$$

$$= F_{t|t} + G_t(F_{t+1|T} - F_{t+1|t}). \tag{91}$$

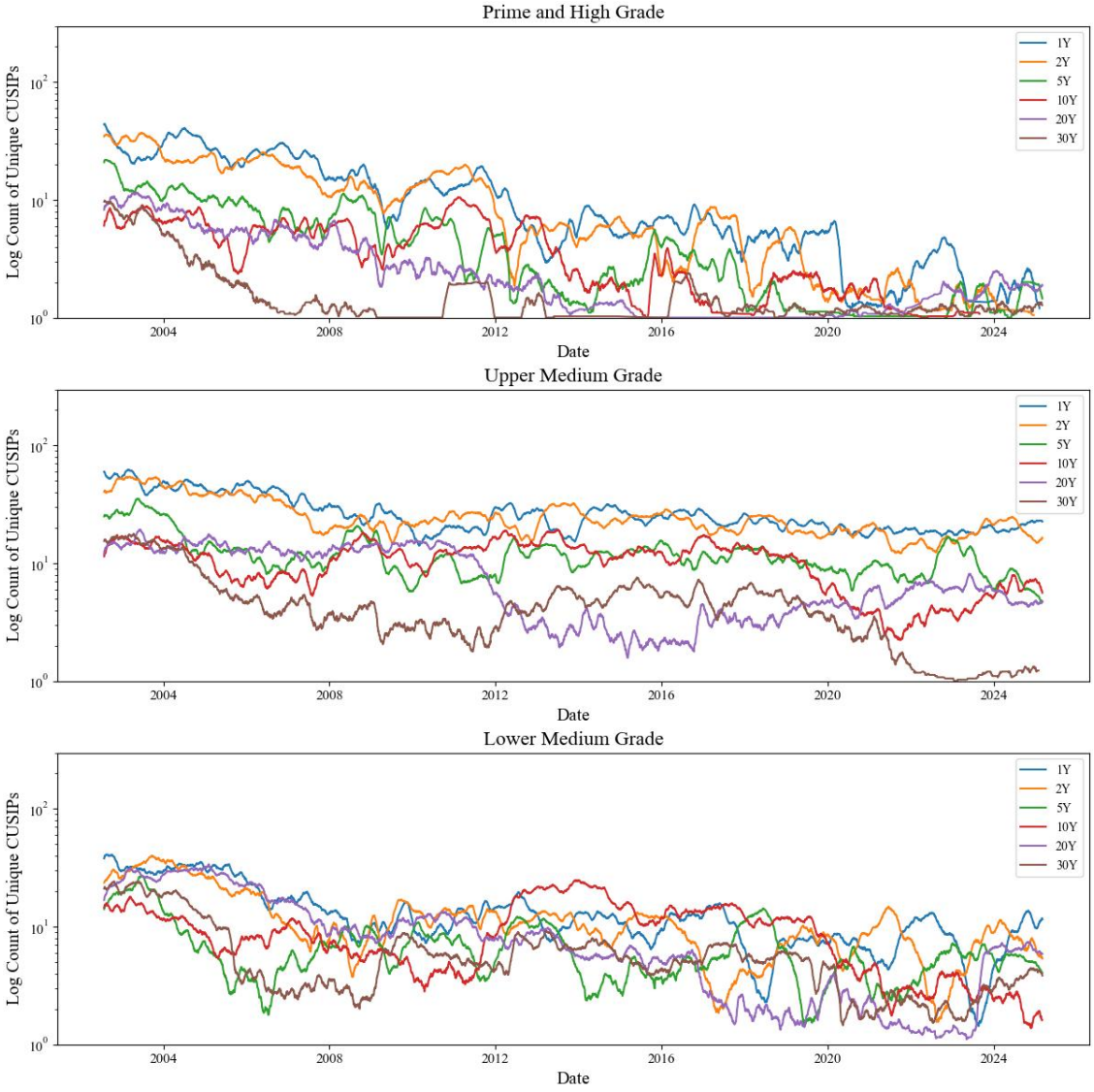
From this, we can recover the estimates of the residuals $\{e_{t|T}\}_{t=0}^{T}$ AND $\{u_{t|T}\}_{t=0}^{T}$ using the following relations:

$$e_{t|T} = F_{t|T} - Af_{t-1|T}, \tag{92}$$

$$u_{t|T} = Y_t - CF_{t|T}. \tag{93}$$

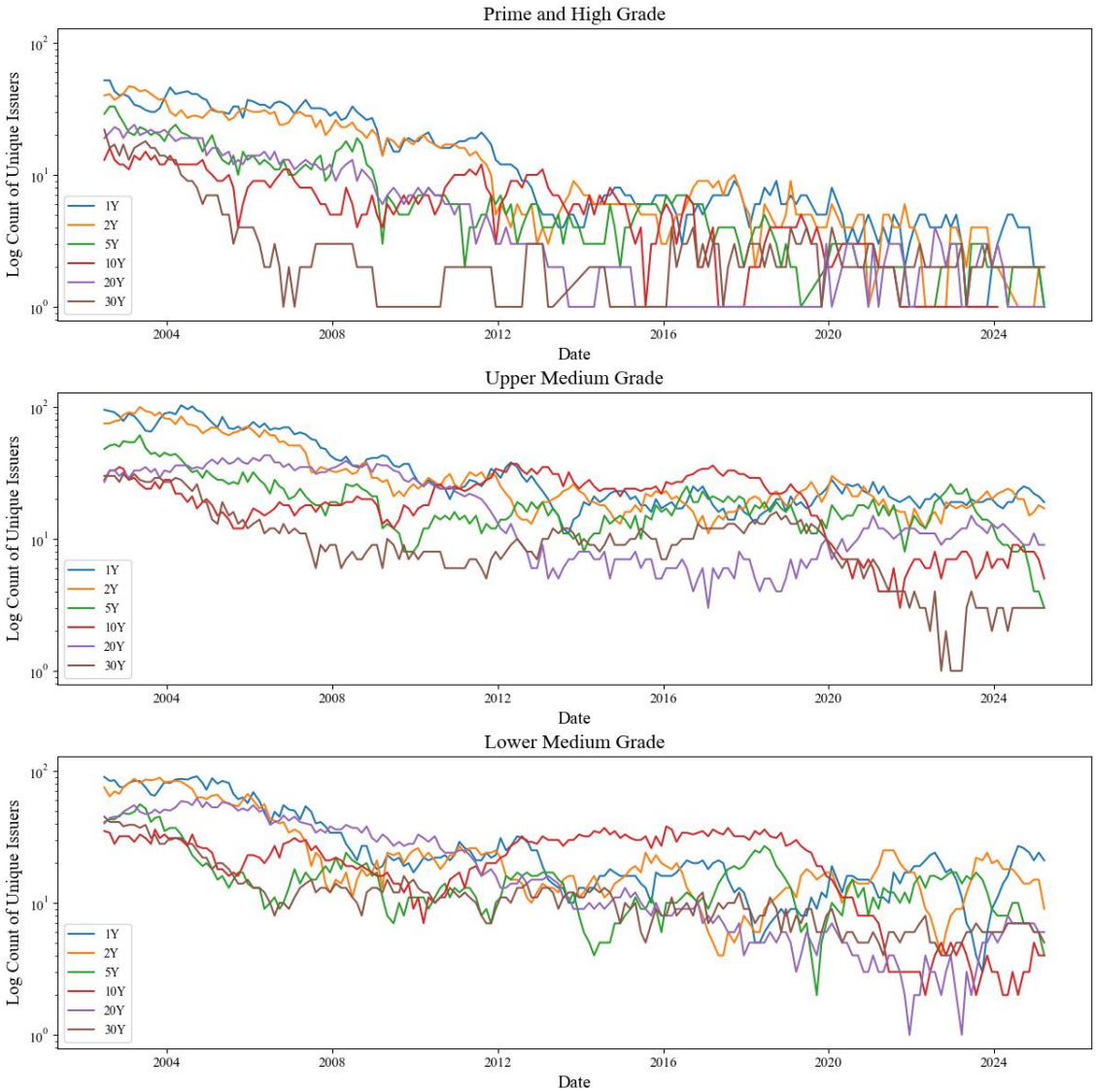
C Additional Tables and Figures

Figure 5: Daily Trading Breadth by Credit Rating and Maturity



Note: This figure plots the rolling eight-week average of the daily count of distinct CUSIPs with at least one trade, separately for Prime and High Grade (top panel), Upper Medium Grade (middle panel), and Lower Medium Grade (bottom panel) bonds. Within each panel, we report selected maturity buckets (1-, 2-, 5-, 10-, 20-, and 30-year). The vertical axis displays the natural logarithm of the number of unique CUSIPs traded. All panels share a common logarithmic scale to facilitate cross-category comparisons. The sample is constructed from TRACE transaction data and spans January 2002 through March 2025.

Figure 6: Daily Trading Breadth by Issuer



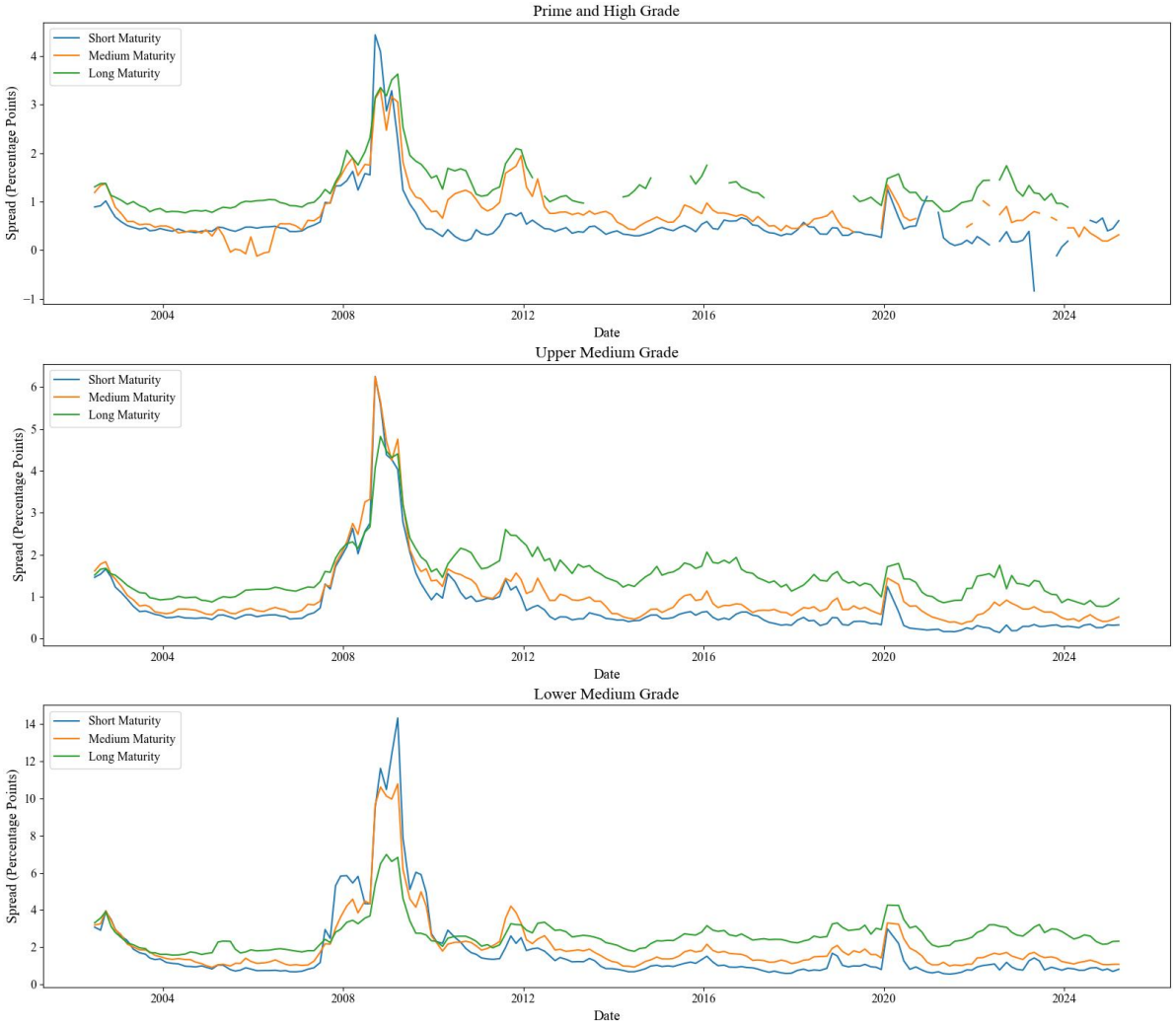
Note: This figure plots the daily count of distinct issuers with at least one bond trade, separately for Prime and High Grade (top panel), Upper Medium Grade (middle panel), and Lower Medium Grade (bottom panel) bonds. Within each panel, we report the 1-, 2-, 5-, 10-, 20-, and 30-year maturity buckets. The vertical axis shows the natural logarithm of the number of unique issuers. All panels use a common logarithmic scale to facilitate comparison across credit categories. The sample is constructed from TRACE transaction data and spans January 2002 through May 2025.

Table 8: Local Projection Estimates of Credit Spread Responses to Monetary Policy Shocks

Horizon (h)	Ps	Pm	Pl	Us	Um	Ul	Ls	Lm	Ll
0	8.49	4.89	3.49	9.94	7.68	5.22	26.9*	17.7	8.43**
	(8.22)	(4.72)	(3.05)	(7.94)	(7.43)	(3.37)	(15.1)	(11.6)	(4.10)
1	-3.32	0.408	2.51	-1.70	-1.95	2.69	7.63	6.12	4.92
	(11.2)	(9.54)	(7.22)	(14.1)	(13.0)	(7.50)	(30.6)	(20.8)	(8.36)
2	1.11	2.88	2.96	3.08	1.70	0.0330	1.74	5.47	3.37
	(12.1)	(10.3)	(8.09)	(15.0)	(14.0)	(9.64)	(35.4)	(25.7)	(12.0)
3	-4.24	2.51	-0.638	-3.17	-2.17	-1.26	4.95	-2.63	-0.501
	(11.0)	(9.84)	(8.85)	(14.3)	(12.7)	(9.11)	(33.0)	(26.0)	(13.9)
4	-5.24	-0.0240	-0.562	-3.54	0.883	-0.794	0.557	-3.37	-0.110
	(9.33)	(10.7)	(9.10)	(12.7)	(12.4)	(8.90)	(39.2)	(27.3)	(15.3)
5	-6.14	-3.55	-1.34	-4.31	-2.38	-1.85	-32.0	-12.0	-4.20
	(6.91)	(6.71)	(6.89)	(8.71)	(10.5)	(7.40)	(29.8)	(21.4)	(13.0)
6	3.34	2.02	1.93	7.35	6.58	0.345	-3.52	7.62	2.79
	(10.0)	(6.53)	(5.99)	(12.3)	(12.9)	(6.49)	(19.3)	(18.2)	(10.9)
7	15.4	7.03	3.04	16.2	13.7	7.33	20.0	26.7	10.4
	(11.2)	(6.56)	(6.18)	(15.9)	(15.9)	(8.21)	(21.4)	(22.0)	(11.7)
8	-6.60	-5.97	-0.556	-9.22	-6.21	0.905	-2.88	1.71	8.01
	(18.4)	(9.05)	(9.31)	(24.8)	(23.2)	(12.6)	(29.2)	(35.7)	(16.3)
9	-1.81	-2.90	0.342	-4.32	-4.12	-2.93	-12.7	-4.39	4.78
	(14.6)	(8.45)	(9.46)	(18.9)	(17.8)	(14.2)	(37.0)	(39.6)	(20.0)
10	6.84	6.42	7.94	4.61	2.96	3.38	26.0	13.3	8.99
	(12.6)	(7.82)	(11.0)	(13.5)	(12.2)	(13.2)	(45.4)	(40.5)	(22.7)

Note: Each cell reports the local projection estimate of the impulse response of credit spreads at horizon h to a one-standard-deviation unanticipated monetary policy shock, with heteroskedasticity-robust (HC3) standard errors in parentheses, based on regression 16. The shock series corresponds to the pure monetary policy component of Jarociński and Karadi (2020). Credit rating categories are Prime/High Grade (P), Upper Medium Grade (U), and Lower Medium Grade (L), and maturity buckets are short (s), medium (m), and long (l). All specifications include three lags (p=3) of yields and spreads ($W_{t-1:t-1-p}$) as controls. Column headers indicate the dependent variable in each regression. Significance levels: *** $p<0.01$, ** $p<0.05$, * $p<0.10$.

Figure 7: Time Series of Corporate Credit Spreads by Rating and Maturity



Note: This figure plots the evolution of corporate credit spreads (in percentage points) from June 2002 to March 2025 across three credit quality cohorts: Prime and High Grade (top), Upper Medium Grade (middle), and Lower Medium Grade (bottom). The spreads are calculated as the difference between the yield of the representative corporate bond and the corresponding maturity-matched Treasury yield. Each panel displays three maturity-based aggregates: short-term (blue), medium-term (orange), and long-term (green). These are defined as the arithmetic mean of the underlying spreads: short-term (1-year and 2-year), medium-term (3-year, 5-year, and 7-year), and long-term (10-year, 20-year, and 30-year). Discontinuities in the Prime and High Grade cohort (top panel), particularly from 2013 onwards, are due to missing data for specific maturities during those periods. Note that the vertical axes are scaled differently across panels to accommodate the varying magnitudes of spread volatility.